Materials for in-vessel components

Gerald Pintsuk [a,*], Giaocomo Aiello [b], Sergei L. Dudarev [c], Michael Gorley [c], Jean Henry [d], Marianne Richou [e], Michael Rieth [f], D. Terentyev [h], Rafael Vila [g]

[a] *Forschungszentrum Jülich GmbH, Institut für Energie- und Klimaforschung – Plasmaphysik, Partner of the Trilateral Euregio Cluster (TEC), 52425 Jülich, Germany*
[b] *EUROfusion Consortium, Programme Management Unit, 85748 Garching, Germany*
[c] *Culham Centre for Fusion Energy, UK Atomic Energy Authority, Culham Science Centre, Oxfordshire, OX14 3DB, UK*
[d] *Université Paris-Saclay, CEA, Service de Recherches Métallurgiques Appliquées, 91191, Gif-sur-Yvette, France*
[e] *CEA, IRFM, F-13108 Saint-Paul-Lez-Durance, France*
[f] *Karlsruhe Institute of Technology, P.O. Box 3640, 76021 Karlsruhe, Germany*
[g] *Belgian Nuclear Research Centre, SCK·CEN, Mol, 2400, Belgium*
[h] *Euratom/CIEMAT Fusion Association, Avenida Complutense 22, 28040 Madrid, Spain*

ARTICLE INFO

ABSTRACT

The EUROfusion materials research program for DEMO in-vessel components aligns with the European Fusion Roadmap and comprises the characterization and qualification of the in-vessel baseline materials EUROFER97, CuCrZr and tungsten, advanced structural and high heat flux materials developed for risk mitigation, as well as optical and dielectric functional materials. In support of the future engineering design activities, the focus is primarily to assemble qualified data to supply the design process and generate material property handbooks, material assessment reports, DEMO design criteria and material design limits for DEMO thermal, mechanical and environmental conditions.

Highlights are provided on advanced material development including (a) steels optimized towards lower or higher operational windows, (b) heat sink materials (copper alloys or composites) and (c) tungsten based plasma facing materials. The rationale for the down-selection of material choices is also presented. The latter is strongly linked with the results of neutron irradiation campaigns for baseline material characterization (structural, high heat flux and functional materials) and screening of advanced materials.

Finally, an outlook on future material development activities to be undertaken during the upcoming Concept Design Phase for DEMO will be provided, which highly depends on an effective interface between materials' development and components' design driven by a common technology readiness assessment of the different systems.

1. Introduction

The performance and reliability of structural, heat sink and plasma facing materials for In-Vessel Components (IVCs), i.e. breeding blanket and divertor including therein incorporated diagnostic systems, is one of the outstanding challenges for the successful development and deployment of nuclear fusion as economically viable future energy source. It is recognized that the very demanding operational requirements the materials will experience in the European Demonstration Fusion Power Plant, referred to as DEMO, and Fusion Power Plants (FPP) beyond DEMO are far beyond today's experience (including ITER). In fact, among the 8 strategic missions defined in the European roadmap to the

realization of fusion energy [1], Mission 3 focuses on the development and qualification of robust materials incorporated into reliable components for the IVCs, able to sustain combined high 14 MeV neutron fluences together with thermal and mechanical loads without severe degradation of their physical and mechanical properties. Within the EUROfusion Consortium, the Work Package Materials (WPMAT) has then been established to tackle most of the objectives set out by Mission 3.

The programmatic objectives of WPMAT have been defined following the recommendations issued in the Final Report of the EFDA Materials Assessment Group (MAG) [2]. One of the main findings of the MAG was that, in parallel to the continued development and

---

qualification of the baseline materials for feeding material data into dedicated handbooks as well as the development of fusion specific design criteria, R&D should be launched towards the development of advanced/risk mitigation materials (RMMs). This aimed at both over-coming possible performance limitations of DEMO (in particular for the second phase – Phase 2 - of operation in which higher dose and accordingly damage will be applied on the materials) as well as extending the operating domain towards conditions more relevant of a future FPP. Moreover, in the absence of fusion-relevant 14 MeV neutron irradiation facilities, irradiation campaigns in fission reactors should be pursued on baseline and advanced materials and complemented by the development of high-level integrated models to qualify and quantify the differences in the neutron energy spectra.

The activities within WPMAT are divided in 6 sub-projects:

- *Engineering Design Data and Integration*

  Material database management, Material Property Handbook, DEMO Design Criteria, Material Technology Readiness Level

- *Advanced Steels*

  Structural material development for low and/or high temperature applications

- *High Heat Flux Materials*

  Plasma facing and heat sink materials including relevant joining technologies for the divertor and breeding blanket

- *Functional Materials*

  Optical and dielectric materials for diagnostics and heat and current drive systems

- *Integrated Radiation Effects Modelling and Experimental Validation*

  Fusion neutron induced material modification and degradation via a multi-scale modeling approach

- *Irradiation*

  Neutron irradiation campaigns for baseline and risk mitigation structural and high heat flux materials

Materials development qualification and validation, as indicated by similar challenges as from fission or Apollo, is expensive [3] and has lead times of approximatively two decades if there is high political and economic interest as well as large industrial involvement while it is expected to be even beyond that for nuclear fusion. Whilst final validation of the materials for DEMO as a nuclear facility with unprecedented loading and damage scenarios will be strongly dependent on the availability of a fusion representative facility like IFMIF, substantial advances on this long path have been made in the field of materials development and qualification via irradiation in material test reactors (MTRs) as well as damage modeling.

The materials development undertaken in the project is aiming at increased collaboration with industry towards upscaling and industrialization as well as international collaborations. This is required to exploit shortfalls in testing capabilities and synergies.

The main developments and achievements obtained in the six sub-projects in the period 2014–2020 will be described in Sect. 2. Sect. 3 presents the plan for future activities to be carried out in 2021–27.

2. Materials topics, highlights and conclusions

2.1. Engineering data and design integration

2.1.1. Objectives

In the DEMO design activity, the establishment of a programmatic link between design progression and material development, i.e. a materials design interface, is crucial. This should facilitate the rapid transfer and integration of advances in material technology and modeling into the concept design activity and the prioritization of design needs and challenges within the development areas of the materials project.

One decisive element in this activity is the development and management of a dedicated and reliable *DEMO materials database* and an efficient data storage system for baseline and advanced materials and the subsequent compilation of a (DEMO) Material Property Handbook (MPH). In view of the reliability of data and material qualification towards nuclear licensing, quality assurance for testing and data generation is of utmost importance, which requires thorough monitoring of information starting at material production via specimen fabrication towards facility and testing parameters. Furthermore, and in view of the expected low amount of data available after neutron irradiation and in particular fusion neutron irradiation using 14 MeV neutrons, the development of suitable statistical data analyses is required to enhance the confidence in existing data and reduce otherwise necessary conservatism in systems and component design.

The MPH should contain information on all design relevant material properties for all baseline materials and those advanced materials that have achieved a sufficiently high materials technology readiness level (MTRL) and proven to be a viable alternative. Thereby, the concept of the MTRL and its periodical assessment allows monitoring advances or obstacles in the development of individual materials as well as identifying gaps towards application in dedicated systems. The latter requires a strong interlink with the technology readiness assessment in systems engineering.

Besides material properties, nuclear licensing of a facility like DEMO requires the development of fusion specific design rules to be compiled as DEMO design criteria (DDC) to enhance the accuracy of design assessments and account for fusion structural integrity assessments. The adopted strategy here is to complement design rules in existing Codes and Standards like ASME-BPVC, RCC-MRx and ITER-SDC. This is done either by adapting and re-writing of existing rules or developing new rules for specific and unique loading cases for nuclear fusion facilities, mainly but not only caused by high-energy, high dose neutron loading, which goes far beyond conditions obtained in nuclear fission and also those expected during the lifetime of ITER. Similar to the assessment of material data, also in the frame of design rules and in view of the large amount of individual components and sub-components to be installed in DEMO, probabilistic approaches for the assessment of material/component damage via dedicated design rules is a pre-requisite for reliable design engineering not only towards nuclear licensing but also for protection of investment.

2.1.2. Achievements

One of the key achievements to date is the establishment of a database that includes over 25,000 carefully assessed and collated individual records from literature, existing databases and the WPMAT testing program [4]. The database covers both baseline and risk-mitigation materials and has steadily evolved since its inception in 2016 (Table1).

This database is the source for the DEMO MPH, for which four incremental releases of the EUROFER97 chapter have been produced and two for optical and dielectric functional materials. In 2020, provisional MPH chapters for CuCrZr and tungsten were released. The MPH represents the best available source of information for DEMO designers, despite the still existing substantial gaps due to a lack of data on properties after irradiation [5]. Moreover, for tungsten and CuCrZr, a

Table 1
Increasing number of database records since 2016.

Material/Sub-project	Records 2016	Records 2018	Records 2019	Records 2020
EUROFER97	>1000	>3000	>3000	No change
Optical and Dielectric materials	2100	7400	>15,000	>16,000
High Heat Flux Materials, covering baseline Tungsten and CuCrZr	300	2600	2750	6650
Advanced Steels	300	2200	2400	6000

significant number of challenges were identified, including but not limited to significant variability in properties between different production techniques and manufacturers and even batch-to-batch variability from the same manufacturer, unknown material specification for the components and unknown requirements for materials properties to validate the designs [3,6,7]. While for CuCrZr the focus will be set in Europe on solution annealed, cold worked and aged materials suitable for the hot radial pressing manufacturing technique in various

conditions representing component manufacturing and operation, particularly for tungsten, the large variability in the material properties does not allow to provide the designers with acceptable materials allowables. Therefore, further collaboration with industry is needed to achieve a clear definition of a reproducible, high quality baseline tungsten material with the focus on rolled tungsten [8]. In 2020 the initial version of the test matrices for tungsten and CuCrZr, both in irradiated and non-irradiated conditions, were produced. They provide a good foundation to base future tests campaigns on and to set priorities in these campaigns thereby allowing an intelligence driven down-selection.

According to the established MTRL methodology [9], all developed materials are characterized by rating them on a scale from 1 to 9, with 9 being the actual system use in DEMO itself. A level of 8 is therefore required for a material being "DEMO-ready" (Fig.1). At present, all baseline materials have achieved levels between 3 and 4, with EUROFER being the most developed. RMMs sit at levels between 2 and 3 pending down-selection and further development, in line with the existing WPMAT strategy. The optical and dielectric functional materials are at slightly higher levels mainly because most are already commercially
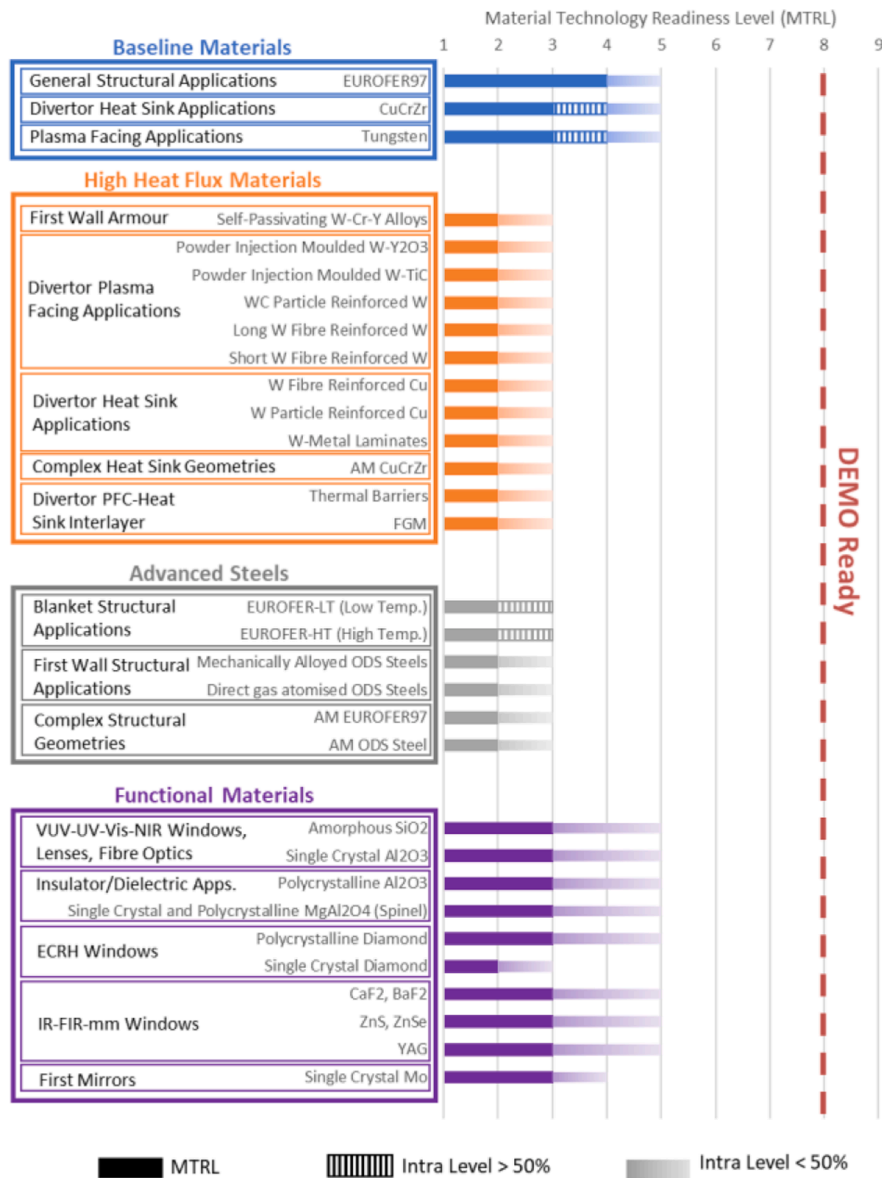

Fig. 1. MTRL of baseline materials, high heat flux materials, advanced steels and functional materials.

available, were and are used e.g. for diagnostic systems in existing fusion devices and neutron irradiation exposure under operation – especially by 14 MeV fusion neutrons – will be lower allowing a better and faster assessment by existing material test reactors and other means like ion beam facilities. However, beyond levels 3–4, the increase of the MTRL for a particular material is intrinsically tied to the design of the system it will be used in, requiring a strong materials-design interface. Accordingly, as the design of the machine progresses, the current MTRL needs to become part of a bigger and comprehensive DEMO technological readiness assessment.

Between 2018 and 2020, the DDC saw key developments, stemming also from the collaboration with industry and interaction with AFCEN experts in RCC-MRx. The content in each section has been rearranged and streamlined aligning it with established conventions in nuclear design codes. Concerning DEMO-specific design rules, development work is performed amongst others on ratcheting, brittle fracture, multi-axial fatigue, exhaustion of ductility and creep-fatigue. Every rule under development now has a dedicated section in where the status can be overviewed and progress tracked. While the rules cannot yet be used to "justify" the design of in-vessel components, they are in a state where benchmark with established methodologies in divertor and breeding blanket design are now possible and have been launched to provide feedback on their use.

Complementary to the commonly used deterministic approaches, work was carried out on defining the amount, and hence quality of the data required to perform probabilistic assessments. This aims in particular on the assessment of an expected reduced number of results after high dose irradiation in material test reactors as well as fusion neutron sources like DONES or IFMIF. Feasibility of the partial safety factor design approach was carried out by an industry project partner Jacobs (formerly Wood PLC) including an example of how this can be applied. This highlighted some limitations in the underlying analytical methods but most importantly uncertainties in the design specifications - such as design loads and their combinations, components geometries and manufacturing tolerances – which prevent for now an effective application of this approach.

2.2. Advanced steels

2.2.1. Objectives

The strategy for designing and licensing divertor and blanket structures is driven by material performance limits and constraints in knowledge. It is currently foreseen that DEMO will utilize a first blanket with a 20 dpa damage limit in the first-wall steel (EUROFER) and conservative design margins and then switch to a second set of blankets with a 50 dpa damage limit with an optimized design (i.e., with somewhat reduced design margins) and, if available, improved structural materials that need to be qualified in advance [10]. The selection of the 20 dpa value as a target for the 'starter' blanket is discussed in [11]. Irradiation of structural materials up to 20 dpa can be simulated, with sufficient accuracy, in existing MTRs, because the level of the He production up to this fluence foreseen in a 14 MeV fusion spectrum is deemed to be still relative modest (~few hundred appm) to significantly affect material properties [11].

It is foreseen that DEMO will utilize for the starter blanket EUROFER RAFM steel and in particular the baseline material EUROFER97. This material was successfully developed with the EU fusion program and has a good overall balance of required mechanical properties (strength, ductility, fracture toughness, creep resistance, fatigue resistance), and there is broad industrial experience in fabrication with production of up to now 4 different batches in the range of several tons each. Furthermore, as a ferritic- martensitic (FM) steel it has a relatively good n-irradiation stability typical of a material with a bcc (body centered cubic) crystallographic structure, i.e. low swelling, and it has been chosen as the structural material for the EU ITER Test Blanket Module (TBM) program, described in Mission 4 of the European Fusion

Roadmap.

However, design windows for materials like EUROFER97 are multi-facetted in a multi-dimensional design space and have to be determined for each design concept individually, in particular as in DEMO a period of operation with a second set of blankets aims for longer life (equivalent to ~ 50 dpa). The most serious risk, with very high impact on any DEMO design, relates to the low temperature embrittlement. The exact low temperature limit, currently derived from fission irradiations, is uncertain because of the added effect of the helium embrittlement from 14 MeV neutrons, but based on available results robust operation of the blanket using EUROFER97 should only be guaranteed if the first wall structure is irradiated above 350°C, even in excess of 20 dpa, but limited to a maximum He-concentration of 500 appm as the brittle to ductile transition (BDT) temperature is strongly sensitive to the helium content (formed by neutron induced transmutation) with a steep gradient at a certain threshold concentration. In combination with a reduction of strength, i.e. softening, at high temperatures, leading to a limit of 550°C, EUROFER97 offers a relatively narrow operating temperature window. There are indications that nano-structured steels, such as ODS-steels, break the 500 appm He limit as the dispersed oxides provide precipitate sites to trap the helium gas and He-gas bubbles generated by high-energy fusion neutron interaction and thus prevent movement to grain boundaries and enhanced embrittlement. Accordingly, they may be used in areas of high temperature and high fluence.

In order to address these issues with the existing options for water or helium cooled breeding blankets, i.e. increase flexibility in the overall reactor design and component lifetime in view of the second phase of DEMO operation ($\leq$ 50 dpa), the main objectives and development lines taking into account that the favorable properties at the respective other end of the temperature window shall be kept are:

- Development of 8–9Cr Reduced Activation Ferritic-Martensitic (RAFM) steels for water-cooled application, EUROFER-LT, i.e. steels with optimized compositions and thermo-mechanical treatments for improved irradiation behavior at low temperature, i.e. 300–350°C, in particular fracture properties.
- Development of 8–9Cr RAFM steels for He-cooled concepts, EUROFER-HT, i.e. steels with optimized compositions and thermo-mechanical treatments aimed at improving the high temperature mechanical properties such as strength, creep and creep-fatigue properties to allow for an extension of the operational temperature range toward 650°C.
- Development of thick semi-finished products for ODS-steels as well as alternative, more simple and less costly Oxide Dispersion Strengthened (ODS) fabrication methods, i.e. development of low-cost ODS fabrication route ("STARS"), both in collaboration with industry with an operational high temperature limit of at least 650°C and an acceptable neutron fluence of at least 50 dpa up to 100 dpa, thus making it a viable option for surface layers in or even main structural material for full First Wall components.

While for LT and HT options, which are all 'classical' steels in general based on EUROFER97, the industrial fabrication development and design integration via various joining/welding technologies should be feasible, the fabrication of ODS-steels is based on powder metallurgy including amongst others mechanical alloying and therefore are more time and cost intensive. In addition, the joining technology is restricted to diffusion welding options.

2.2.2. Achievements

More than 50 new alloys, of either EUROFER-LT or EUROFER-HT variants, were successfully cast since 2014. Two strategies and a combination thereof were followed to optimize the materials micro-structure and improve the mechanical properties at either end of the temperature window: i) performing modified/additional thermal or thermo-mechanical treatments (TMTs) on standard EUROFER; ii) modifying the

chemical composition.

For EUROFER-LT, reduction of the DBTT w.r.t. the band of about −100°C to −60°C for standard EUROFER was already obtained for several alloys in the non-irradiated conditions (Fig.2).

The microstructural and mechanical characterization of selected properties in non-irradiated conditions allowed for a first down-selection followed by a screening irradiation campaign in the HFIR reactor at ORNL, US, on a selected number of alloys in the low temperature regime (see Section2.5 [14]). Among these alloys the most promising material is a 'lab-cast EUROFER' [15], produced with alternative TMTs. These resulted in a BDT temperature already before irradiation of −147°C, based on the KLST Charpy impact test results, while maintaining similar tensile properties as EUROFER97/2 in the high temperature application region, and accordingly provides also the lowest value of the fracture toughness transition temperature (FTTT) after irradiation. Therefore, this material can be considered as the optimum state of EUROFER in terms of fabrication, TMT and HT. Detailed material characterization and upscaling of this production route will be the focus of further R&D in the future. An alternative approach is equally being followed by investigating the effect of cold working plus tempering on standard EUROFER and modified RAFMs subjected first to a double austenitization, quench and tempering treatment [13]. Due to their ultra-fine grain size, the recrystallized materials are expected to have a higher radiation resistance compared to standard EUROFER. At the same time, welding of these materials proves to be difficult which is another criteria in the selection process. To support the down-selection process, a technological assessment and further irradiation campaigns are needed.

The results for EUROFER-HT show that the development of 9Cr steels for HT applications is a realistic goal. In contrast to the LT variants, the down-selection process requires a further significant amount of information and accordingly a larger number of materials is still under consideration. One promising option are RAFM steels with W contents up to 3 wt% and with isotopically tailored B additions avoiding additional He-transmutation/generation under neutron irradiation [16]. In particular, the creep test at 650°C/100MPa for the 3 wt% W and high B alloy showed a final creep lifetime of 13,123h, the highest value measured so far for alloys investigated as part of the DEMO Programme (Fig.3). The addition of B however induced a degradation of impact properties at low temperature. Alternative heat treatments as well as alloys containing no B are being investigated to avoid this problem.

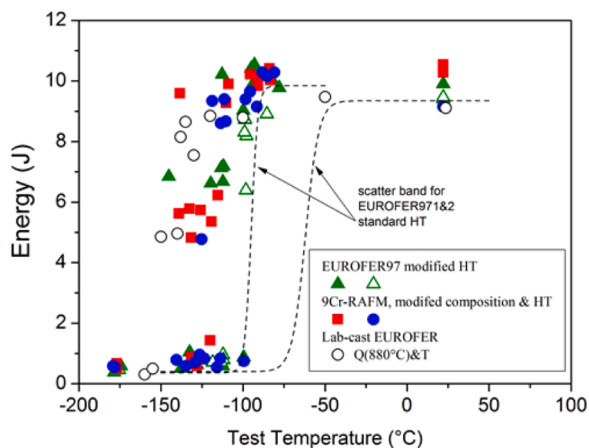Another approach in the HT regime is the development and use of a

Fig. 3. Creep tests performed at 650°C on 9Cr RAFM steels with various W and B contents.

computational model for the selection of chemical compositions and heat treatments optimized for improved high temperature properties. A "high throughput" screening of different tempering time-temperature combinations was launched, leading to a selection of three material/heat treatment combinations providing the best mechanical properties that will be further investigated.

Finally, for the development of ODS steels, one major accomplishment was the fabrication and testing under representative heat-fluxes of a He-cooled First Wall mock-up with ODS plating (Fig.4, [17]). The ODS plates were produced from mechanically alloyed powders with a final chemical composition of Fe-13Cr-1.1W-0.3Ti-0.3Y2O3, consolidated by HIP and then tempered and hot-cross-rolled to the final thickness. The plates where then HIP-bonded to a massive base plate of EUROFER97/2 and cooling channels were machined after HIPing. The completed helium-cooled FW mock-up was tested in the HELOKA facility at the Karlsruhe Institute of Technology (KIT) under FW-relevant heat-loads. Under such conditions, the surface temperature was close to 650°C. The helium cooled mock-up successfully completed the tests without any visible structural damage (Fig.4).

Further developments of ODS materials would require the manufacturing of even larger/thicker material pieces in order to allow replacing EUROFER for the whole plasma facing unit by the ODS-steel. A new task was started in 2019 with the aim to evaluate whether full first wall components could be made of ODS. Five ODS grades, with Cr contents ranging from 9 to 14%Cr and therefore martensitic to ferritic, were designed and produced using the same industrial route. Microstructural and mechanical characterization are on-going. In parallel, ODS production by alternative routes using mechanical alloying by atomization processes and reaction synthesis is being investigated [18]. Significant advances were achieved by the successful production at industrial scale of high quality powders containing Y and Ti, from which ODS capsules were produced. However, the mechanical strength of ODS produced with the new route still needs to be improved. Additional activities regarding rolling parameters and subsequent heat treatments should be carried out to increase the density of dislocations during rolling, enhance dissolution of metastable phases and promote the precipitation of oxide nanoparticles.

2.3. High heat flux materials

2.3.1. Objectives

This class of materials consists of plasma facing materials for the divertor and the breeding blanket, heat sink materials to be used in the divertor region and interfaces between these materials, as well as joints. The latter are aiming for creating components with an improved structural stability under the operational thermal and neutron loads with a sufficiently high heat removal capability.

Tungsten is the baseline material for state-of-the-art technology in plasma-facing components, mainly because of the high threshold energy

Fig. 2. Charpy impact test data (KLST) for optimized RAFM steels in comparison to EUROFER97 1 & 2 and standard heat treatment (HT); a) modified HT (triangles): double austenized and tempered commercial EUROFER in L-T (full) and T-L (open) orientation; b) modified composition and HT [12]: double austenized and tempered EUROFER with high Ta (square) and low Ta (circle) content [13].
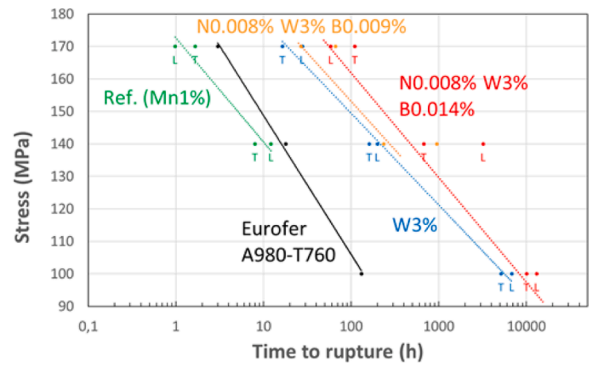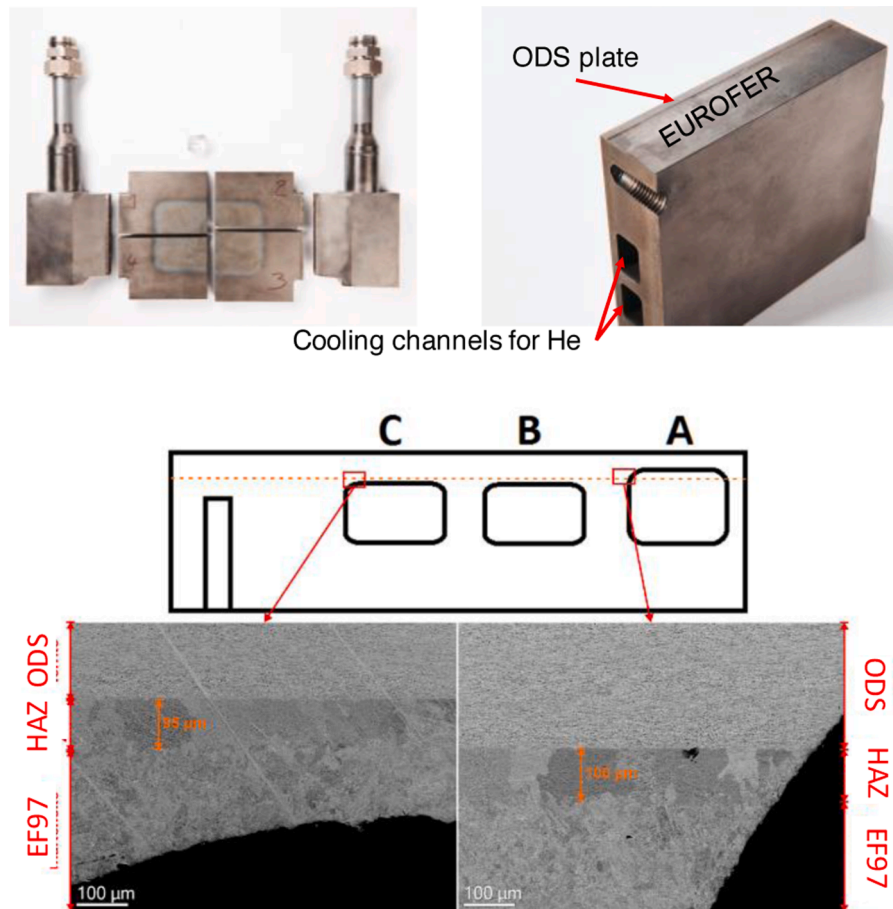
Fig. 4. ODS-EUROFER FW mockup cut up after testing and SEM analysis at the interface of the HIP joint – transition from ODS plating (thickness=3mm) via the heat affected zone (HAZ) to EUROFER97 (thickness=20.5mm); total size of ODS plated area: 200×160×23.5mm.

for sputtering by hydrogen isotopes (around 100–200eV), the low retention of tritium in the material and its high melting temperature [19Pintsuk]. However, drawbacks related to tungsten are its intrinsic low temperature brittleness, neutron induced embrittlement and recrystallization resistance. On the one hand, neutron embrittlement in pure tungsten, exposed to ∼ 2–6 dpa per full power year [20,21] in divertor plasma facing components, occurs up to irradiation temperatures of at least 600–800°C; this requires further studies due to a lack of irradiation data and is strongly limiting the safe low temperature operational range. On the other hand, recrystallization and related material softening leads to increased susceptibility to thermal fatigue induced damage formation, which is expected to determine the upper limit [22] (typical value for ITER grade tungsten: ~1300°C). Furthermore, in view of accidental scenarios including a loss of cooling combined with water and/or air ingress, tungsten has low self-passivation capabilities and will experience excessive erosion and formation of volatile radioactive tungsten oxides [19].

For the heat sink materials in the divertor, CuCrZr is the actual baseline material for DEMO and also the material of choice for components in ITER. CuCrZr has a limited operational temperature range due to neutron induced reduction/loss of uniform elongation at temperatures below 180–200°C as well as irradiation induced softening in the temperature range from 300 to 350°C, both requiring further investigations, in particular at high neutron fluences and damage levels of 5–10 dpa, which is in the range of the expected neutron damage within 2 full power years for the divertor strike zone region [20].

In order to address these issues with baseline tungsten and CuCrZr the sub-project HHFM is dedicated to the material development and characterization of improved and novel plasma facing and heat sink materials as well as joints and interlayers between these mainly for divertor applications but also to a minor extent for applications at the first wall blanket. The developed materials and data generated provide the input to the design of the divertor and breeding blanket. Further work on W involves plasma-wall-interaction studies primarily oriented towards the exposure of the materials to hydrogen and helium particle loads at various temperatures.

Accordingly, the R&D on high heat flux materials will focus on the following main topics:

- Development and optimization of tungsten-based armor materials with improved a) fracture toughness tackling the low-temperature neutron embrittlement with the goal to close the yet existing gap in the operational temperature window between plasma facing and heat sink materials aiming for < 600°C, ideally 450°C; b) recrystallization resistance and related resistance to thermal fatigue to increase material lifetime under the expected thermal loads in the range of up to 20 MW/m^2 in the strike point region; c) oxidation resistance in particular for applications at the First Wall or for regions with reduced heat flux in the divertor relevant under accidental conditions, in particular during a loss of coolant accident (LOCA).
- Development and optimization of Cu-based structural materials and composites using particle and fiber reinforcement, quaternary alloys, ODS strengthening as well as innovative laminate structures fully or partially made from tungsten for improving the high temperature mechanical properties such as strength, creep and creep-fatigue to improve neutron resistance at low temperature down to 150°C corresponding to the expected coolant temperature for plasma facing

- components in the divertor and increase the upper operational temperature limit to at least 450°C.
- Development and optimization of innovative interlayer materials like functionally graded materials (FGMs) or thermal barrier layers as part of advanced design concepts for the mitigation of thermally induced stresses using different approaches.

The final qualification of the materials needs to be performed by manufacturing and testing high heat flux test components mock-ups to demonstrate their technical maturity.

2.3.2. Achievements

2.3.2.1. Plasma facing materials. Building on programs launched more than 10 years ago [23], the R&D program has focused on the qualification and maturation of materials design and manufacturing technologies towards industrialization and large scale production. One route thereby is the use of carbide and oxide particle reinforcement for increasing strength and recrystallization resistance. Several tens of new tungsten materials and composites (pure W acting as reference as well as with additions in the range of 0.5 – 8wt.% of W_2C as well as TiC, TaC, La_2O_3, Y_2O_3, HfC, HfO, *Re* and combinations thereof with varying particle size) were produced via various sintering techniques and powder injection molding (PIM) [24], a near net shape technology requiring no subsequent mechanical treatments like forging or rolling. Microstructural, mechanical as well as characterization via the application of operationally relevant transient heat loads have shown that the benefit of these materials is clearly on the high temperature side, i.e. in the range of the first few millimeters close to the plasma facing surface with an improved recrystallization as well as thermal shock induced thermal fatigue resistance [6]. However, in the low temperature regime, no improvement or even further degradation in view of materials ductility compared to pure reference tungsten materials have been observed, which would require the combination of these particle reinforced materials with materials produced via other material fabrication technologies, i.e. including material deformation, for the fabrication of the foreseen monoblock components. As this does not comply with the intention and strength of PIM this route has been, supported by screening irradiation results discussed in Section 2.5, finally discarded. In addition, oxides and in particular carbides at the plasma facing surface provide a potential impurity source leading to material migration and deposition/co-deposition and need a more detailed assessment on allowed quantities.

A second route is the development of tungsten-fiber reinforced tungsten composites using two variants, (i) long fiber reinforced composites produced via chemical vapor deposition (CVD) and (ii) short fiber reinforced composites produced via field assisted sintering techniques (FAST) in combination with a final densification via hot isostatic pressing (HIP) [25–27]. These materials with highly ductile and high temperature/recrystallization resistant potassium doped tungsten fibers and a pure tungsten dense or porous matrix are aiming and have proven to overcome the low temperature brittleness by introducing a pseudo-ductile behavior using the different mechanisms of fiber reinforcement, i.e. fiber pull-out or crack deflection at fibers, and thereby avoiding catastrophic brittle failure. Thereby, the combination of fiber or braided fiber yarns (Fig. 5), matrix and novel developed interfaces like Y_2O_3 is decisive to take benefit of the mentioned processes. However, while for short fiber materials with randomly oriented and individually coated tungsten fibers in the range of ~2.5mm there is a higher flexibility in matrix composition due to the used sintering processes, the random orientation and the comparably short fibers reduce the beneficial effect compared to the long fiber variant. In both cases the main issue to overcome is the industrial upscaling, which requires continued increased effort and led to the decision to not consider this material for the application in the start-up of DEMO but treat it as high potential
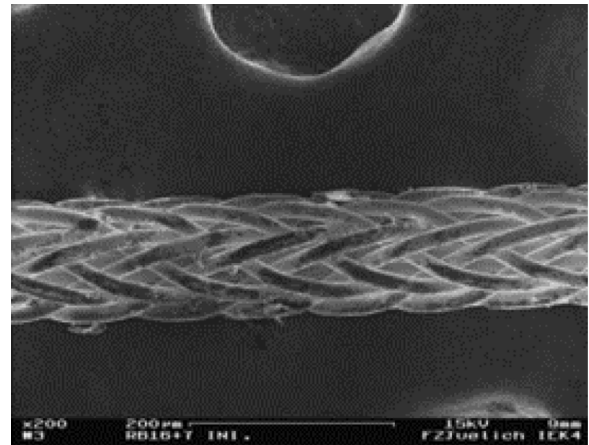

Fig. 5. Braided fiber yarn (16+7 filaments).

material for application in fusion devices beyond that.

Additional alternatives include tungsten/tungsten laminate structures using the combination/joining of numerous thin cold rolled foils, which provide high ductility and the shift of the brittle to ductile transition temperature to values below room temperature due to nanostructuring [28]. While via this route highly ductile material can be produced in the low temperature regime, the drawback is a low recrystallization temperature below 1000°C due to the high stored energy. One potential option to overcome this issue is the use of potassium doped tungsten materials for foils but also for thicker plates [29,30]. While the reinforcement mechanism applied by potassium doping works best in fibers, application of potassium doping in combination with (cold) rolling processes still requires further analyses despite very promising irradiation results shown in Section 2.5.

Finally, self-passivating tungsten alloys containing Cr as oxide forming element as well as an element that stabilizes the oxidation process (e.g. Ti, Y or Zr), are meant to be used as plasma facing material for the first wall. This is to minimize the risk of forming a vast amount of volatile tungsten oxides in case of a loss of coolant accident (LOCA). These materials have been successfully produced on the lab-scale via mechanical alloying to obtain the required fine distribution of elements followed by either HIP or spark plasma sintering (SPS) [31,32]. The materials with a clearly defined ternary (W-Cr-Y) and quaternary (W-Cr-Y-Zr) material composition provide an increase of the oxidation resistance by up to a factor of 10^6 in a temperature range up to 1000°C in dry and humid atmosphere. While still providing an increased brittleness compared to the other developed tungsten composites, they have shown increasing mechanical stability and comparable resistance under transient thermal loads. The next step to be undertaken is, besides continued efforts to further improve the mechanical performance, the industrial upscaling of the manufacturing process. The focus thereby will be set in particular on the reproducibility of the achieved and required powder quality produced via mechanical alloying at the lab-scale, which is essential for the fabrication of high performance materials.

2.3.2.2. Heat sink materials. The most developed and already industrially available heat sink material for water cooled applications is tungsten particle reinforced Cu and CuCrZr [33,34] with preference on CuCr or CuCrZr in view of the increased amount of swelling of pure Cu under neutron irradiation. In comparison to CuCrZr it shows a significantly improved mechanical performance (strength, fracture toughness) and stability in the non-irradiated state up to temperatures of 500–550°C.

The second option, i.e. W-fiber reinforced Cu and CuCrZr outperforms the particle reinforced material in terms of strength and ductility in the whole temperature range in the non-irradiated and irradiated case (see chapter 2.5). This material is developed in

collaboration with industry and has been produced in the shape of plates and tubes [25,33]. Thereby, woven tungsten fiber fabrics using fibers with varying thickness and volume density were used that are subsequently liquid melt infiltrated and thermally treated. Further upscaling of the industrial production route is required.

For both strategies, particle and fiber reinforcement, ITER shaped mock-ups with a dedicated cooling tube fabricated from the novel materials were produced, which survived in the non-irradiated state high heat flux testing at 20 MW/m^2 without indication of failure. In view of the better performance of the fiber reinforced material this material has been selected as the primary candidate, leaving the particle reinforced material only as back-up option.

For He-cooled applications, i.e. higher coolant temperatures, tungsten laminates are aiming for a ductilization of tungsten [35]. Laminates were produced in the form of plates and tubes using ductile tungsten foils with interlayers of Cu, CuCrZr, Ti and V. While all materials show ductile behavior at room temperature in the non-irradiated state, strong emphasis has to be put on the materials interface and the long term stability under operational conditions. Thereby, Ti and V are prone to react with tungsten and for the use of these materials, additional thin interlayers, e.g. Cr or Cu, are required. However, irradiation campaigns up to 1 dpa at different temperatures have shown that the laminates undergo strong embrittlement and therefore this material which provides high strength and ductility for non-irradiated applications, has been discarded for the use in a neutron environment.

Besides these "conventional" approaches, additive manufacturing technologies using laser beam melting were investigated, exploring the modeling and CAD (computer aided design) based development of complex tungsten matrix structures which will subsequently be infiltrated by pure Cu or a Cu-based alloy substituting the heat sink material and providing a better adjusted thermal expansion coefficient to the plasma facing material while still featuring high thermal conductivity. In contrast to the conventional monoblock design the strategy here adapts the flat-tile design (Fig.6) [36].

2.3.2.3. Interfaces. Both thin ($\sim$15μm) and thick ($\sim$0.5mm) W/Cu-FGMs have been successfully produced via PVD and plasma spraying, respectively, as well as characterized. Accordingly, the technology development has been finished and is readily available for being used in divertor concepts. These FGMs were successfully used and tested up to 500 and 1000 cycles at 20 MW/m^2 in mock-ups built according to the ITER-like monoblock design using than and thick FGM configurations,
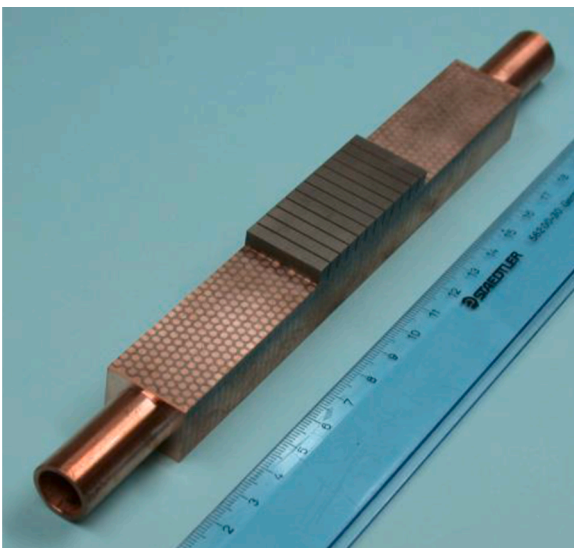

Fig. 6. Tungsten flat tile component with additively manufactured heat sink (Cu-infiltrated W-honeycomb structure).

respectively [37,38] and in the course of the optimization of the component manufacturing process issues with either crack formation at the interface, such as for the baseline DEMO divertor ITER-like concept [39], or softening of CuCrZr during the manufacturing process evolved and have been tackled by various means. The final qualification of the optimized components via high heat flux testing is still pending. A final selection of this technology depends on the figures of merit, i.e. the achievable performance under cyclic heat fluxes, compared to the complication/increased cost of component manufacturing.

For a very particular design option relying on a more homogeneous temperature distribution with the component, thermal barrier materials are developed using flexible amounts of oxide and carbide additions to Cu (e.g. SiC, ZrO2, C) [40,41]. These were fabricated using FAST and exhibited thermo-physical properties tunable over a wide range, i.e. from pure Cu at $\sim$ 400W/m.K down to a few W/m.K. The fabrication of suitable inserts/rings for an optimized monoblock design based on FEM-analyses and consisting of several different materials adapting an FGM-like structure has been performed as well as their implementation into mock-ups. The proof of principle to be done via high heat flux testing is still pending and while the material development has been finished no selection or down-selection could have been performed yet.

Finally, joining technologies for newly developed materials were investigated addressing in particular the joint between the self-passivating plasma facing material and EUROFER in the high heat flux components of the first wall. This comprises brazing as well as diffusion bonding with the focus, but not exclusively, on pure Cu and Cu-based interface layers. In both joining processes elemental diffusion takes place, nevertheless the obtainable shear strength values of the brazed joint reach appreciable values > 340MPa [42].

2.4. Functional materials

2.4.1. Objectives

Functional materials like tritium breeders or neutron multipliers, permeation barriers etc., are part of the R&D conducted in the Work Package Breeding Blanket (WPBB). However, some of these materials, i. e. dielectric, optical and mirror materials used predominantly for diagnostics and control as well as for heat and current drive systems that may also be used in the breeding blanket and divertor as insulator materials, were included in WPMAT to avoid duplications in material development.

The degradation of functional, physical and, to some extent, mechanical properties of this material class leads to severe limitations for their applications in DEMO. This degradation that appears at very low doses, seriously compromises the lifetime and accuracy of all the basic heating and control systems. The investigation and characterization of the present industrially available candidate materials as well as new developments are to be extended to include representative DEMO reactor conditions including characterization under neutron irradiation up to damage levels of 1 dpa.

The following different topics covered in this sub-program are:

- Characterization of the effect of self-ion and He irradiation on reflectivity with the focus on polycrystalline and single crystal Mo-mirrors including development and characterization of nano-grained materials.
- Development and optimization of optical materials as well as characterization of industrially available materials including silica, sapphire, YAG, spinel and diamond for control and safety. Reproducibility and radiation hardness, i.e. high optical transmission under both, neutron and gamma irradiation, are the main drivers to allow the selection of candidate materials for application in the visible as well as the infra-red range.
- Development and optimization of dielectric materials for diagnostic and H&CD applications, e.g. diamond windows using polycrystalline and single crystal diamond, as well as characterization of industrially

available materials like alumina and silica. Reproducibility and radiation hardness in terms of loss tangent as a function of frequency and irradiation temperature and dose are the main drivers to allow the selection of candidate materials.

- Development of multiscale models applied predominantly to alumina to understand long term degradation of optical and electric properties. This is the best known material under radiation with a large amount of experimental data for comparison.

2.4.2. Achievements

2.4.2.4. Optical materials. Ion irradiation studies of Mo mirrors have shown that the main influencing parameter on the reflectivity is not the damage formation in the optically active surface near layer of 20nm induced by self-ions used as proxy for neutron irradiation but the formation of He-voids in the surface near region (caused by He implantation) and the deposition of surface layers induced by material migration. It has been demonstrated that the microstructure of the material has almost no influence on the He-induced degradation and if at all, a nanometric grain size causes a further decrease of reflectivity (Fig.7). By the combination of He and subsequent H irradiation, due to the increase number of trapping sites, the H retention increases by almost a factor of two as well as the retention depth increases. Studies on material migration, i.e. W-deposition, have shown that it has an additional
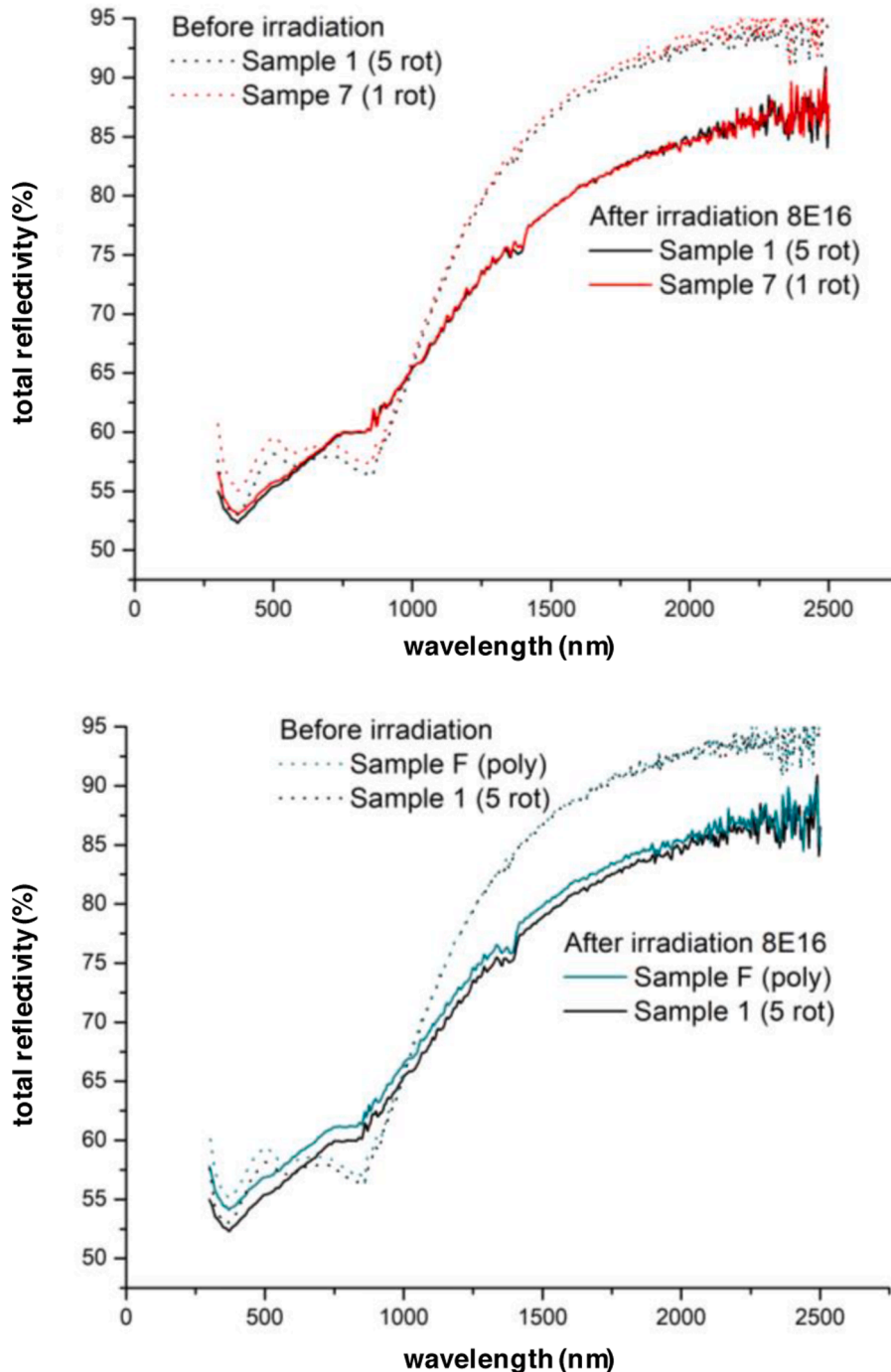

Fig. 7. Total reflectivity of polycrystalline Mo-mirrors before and after irradiation with He+ ions: comparison of materials using severe plastic deformation via high pressure torsion with different rotations (top); comparison of industrially available (poly) and severe plastically deformed materials using 5 rotations (bottom).

detrimental effect causing a reduction in the visible range by 30–40% and in the infra-red range by another 5%.

Optical materials for windows have been extensively studied under neutron/gamma irradiation and for a selected number of 12 materials an irradiation campaign has been launched for obtaining damage levels of 0.1, 0.4 and 1 dpa (fluence of $1 - 10^{24}$ n/m^2) at a temperature of 250°C. For all investigated materials (amongst others MgAl$_2$O$_4$ spinel, silica and sapphire) a clear increase in optical absorption has been observed with the lowest degradation found for silica in the UV–VIS-NIR range. The same applies for silica under in-situ gamma irradiation after neutron irradiation demonstrating that silica can accommodate neutron damage in a relatively efficient way, with an excellent self-healing of optically active centers [43]. The same applies for sapphire in the infra-red range (3–4μm) showing there hardly any degradation and making those two materials the selected candidate materials for diagnostic windows in the respective wavelength range. In contrast to those materials, diamond samples became completely black after neutron irradiation losing all its optical transparency. Accordingly, it has been discarded as optical material. The same applies for yttrium aluminum garnets (YAG), which showed a comparably large increase in optical absorption and therefore was also qualified as not radiation resistant enough for optical applications. Finally and in contrast to ion irradiation studies, C12A7 single crystal materials undergo drastic changes in the region of fundamental absorption under neutron irradiation and although regarded as promising based on earlier results has been discarded. Finally spinel materials demonstrated a lot of variations between samples, as they show important recovery during the hours/days after irradiation.

2.4.2.5. Dielectric materials. Within the same irradiation campaign also comprising the optical materials, a number of different dielectric materials were investigated including 3 different grades of amorphous silica as well as two versions of differently produced alumina with very high purity [44].

The dielectric properties (tan δ and ε) were measured using 3 different systems, at room temperature in the range of 1kHz to 13GHz, before and after neutron irradiation. Silica thereby presents "saturation" of degradation starting already at the lowest investigated neutron fluence. This could be attributed to a saturating damage due to the amorphous structure and indicates a reduced importance of the silica origin at high doses. It further demonstrates that final material qualification must be done as close as possible to operating conditions. To understand this crucial effect, further irradiation campaigns are needed.

For the alumina samples, Fig.8 shows the observed increase in the loss tangent values after neutron irradiation in the kHz to MHz frequency range. At lower frequencies, there is monotonic increase of loss, although quite moderated. In the MHz range the difference between 0.1 and 0.4 dpa becomes smaller and further data on 1 dpa should reveal if a similar saturation effect is observed, as found for silica.

Besides these studies on ceramic dielectric materials, a special case diamond has been investigated for ECRH (electron-cyclotron resonance heating) devices. To reduce losses for microwaves in different power levels in diamond windows, single crystalline diamond is the material of choice, because there is no Rayleigh scattering at grain boundaries in such crystals. As the maximum size of diamond single crystals is still limited to few centimeters by the available fabrication processes, cloning of single small diamond chips was investigated. A verification of single-crystallinity was performed by using EBSD (electron back-scatter diffraction) showing that crystallographic order (high cubic orientation) is well preserved, with only small deteriorations near the interface area. Furthermore, new techniques like thin film resonators were developed to investigate the permittivity and loss tangent on small specimens.
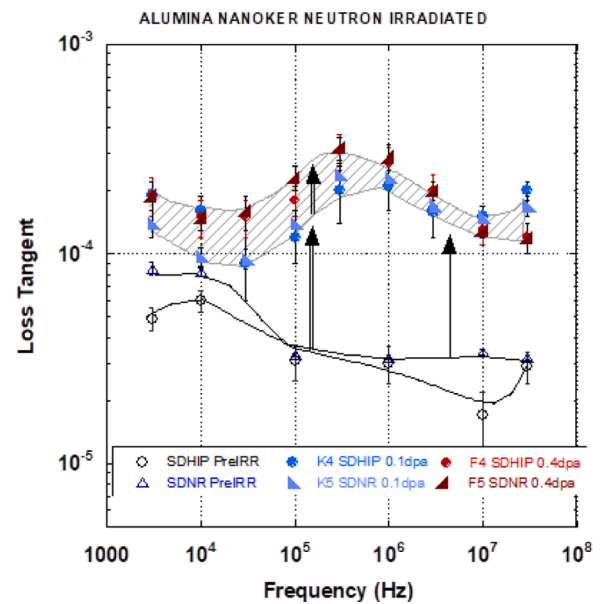

Fig. 8. Comparison of loss tangent of the present neutron irradiated alumina samples with unirradiated reference materials.

2.5. Irradiation

2.5.1. Objectives

One of the major objectives in WPMAT was to carry-out neutron irradiation studies as neutron irradiation is an indispensable tool not only for the determination of material properties but also for the qualification of newly developed materials. In line with the DEMO development plan and the available irradiation facilities, the priorities are on the determination of materials data for the DEMO blanket starter configuration (i.e. material data up to 20 dpa [10]), which is characterized by irradiation hardening with limited transmutation damage and is of highest priority. Irradiation of materials with neutrons in fission reactors includes two complementary issues:

- Collect data and optimally fill database gaps for the baseline materials EUROFER97, tungsten and CuCrZr to support component design, in particular with respect to mechanical properties.
- Generate data for risk mitigation materials development and selection and for the understanding of the basic material behavior including its validation.

In addition, one major topic is the planning and preparation of irradiation campaigns in MTRs for baseline and advanced materials under DEMO relevant loading conditions in terms of neutron fluence and operational temperature for the second phase of DEMO operation (> 20 dpa; study of He-effects).

2.5.2. Achievements

In 2016 and 2017, eight irradiation campaigns were launched in total and their objectives and specifications as well as the expected end dates are given in Table2. Three campaigns were dedicated to fill in gaps in the materials database (LOT-I, II, III). Four campaigns (LOT-IV, VII, A, B) contributed to the future direction of material development lines by screening advanced materials (steels, composites, heat sink, and tungsten alloys) while one campaign (LOT-IX) delivered data for tungsten model validation. It should be noted that six of the campaigns are performed in two European facilities and two campaigns could be realized in partnership with the US Department of Energy and ORNL. In this way, the European program benefits both from the US high flux reactor and from the investment into the upgrade of existing European facilities.

Table 2
Neutron irradiation campaigns launched within EUROfusion WPMAT.

	Campaign	Material	dpa	T [°C]	Property	End of irrad. / PIE
LOT I	Blanket Baseline Design	EUROFER	20	200–350	Tensile, toughness, R-curves	May-2021 / 2022–2023
LOT II	Divertor Baseline Heat Sink Design	CuCrZr	5	100–300	Tensile, toughness, LCF	Jan-2021 / 2022–2023
LOT III	Tungsten Basics	W	1	400–1200	Toughness	Jun-2018 / 2021–2022
LOT IV	Screening of Advanced Steels	9% Cr steels	2.5	300	Tensile, toughness	Apr-2018 / completed
LOT VII	Screening of HHF Properties	W composites	1	600–1200	Thermal shock and plasma loading	Sep-2018 / 2021–2022
LOT IX	Validation Data for W Modelling	W	1	600–1200	Hardness, strength	Dec-2017 / completed
LOT A	Screening of heat sink materials	Cu alloys / composites	1 (W)	150–450	Tensile	Mar-2019 / 2021
LOT B	Screening of plasma facing materials	W alloys / composites	1	600–1100	Bending, BDT	Mar-2019 / 2021

Of these eight irradiation campaigns, six campaigns (LOT I, II, III, IV, VII, IX) were officially started in June 2016. Two additional irradiation experiments (LOT A and B) were initiated by end of 2017 and launched in 2019. From these, LOT-IV and -IX were completed including PIE (post-irradiation examination). The Lot A, and -B PIE work is far advanced so that the main trends are recognizable. Therefore, important conclusions for the design and for planning the future program direction can be drawn. PIE of the LOT-I campaign had to be postponed to mid-2021 due to a reactor outage and PIE of LOT-VII can only be completed after the installation of the HHF hot cell test facilities in FZJ. LOT-II had to be completely restructured due to an erroneous rig design. Therefore, the initial objectives had to be canceled and replaced by much less relevant goals. The related PIE will be launched in 2021.

2.5.2.1. Lot III. The goal of the Lot III campaign was the provision of tungsten irradiation-hardening/DBTT (ductile to brittle transition temperature) behavior within the operating temperature limits of armor parts. The lower operating temperature in current designs varies between 400°C and 600°C, which was therefore used as the lower irradiation temperature. Irradiation in the high temperature regime (800–1200°C) was aimed at the determination of the onset of defect annealing. The project included a very well characterized pure forged W grade from Plansee AG (IGP).

Even at very low doses, a significant shift in DBTT can be observed for the samples irradiated at 600°C, which was expected for such low temperatures (i.e., $T \ll 1000°C$). Further preliminary test results for all irradiation temperatures indicate an influence on the DBTT as compiled in Table3.

A first interpretation for the obviously missing recovery behavior with rising irradiation temperature is a complex interplay of irradiation defects: (1) hardening by the irradiation induced lattice defects (interstitial clusters and dislocation loops), (2) vacancy clusters and voids, and (3) transmutation products (Re, Os). Each of these three elements may have a different temperature dependency and, moreover, they will most probably influence each other's formation dynamics.

This interpretation is also supported by hardness test results, which show that the recovery is not fully reached even at 1200°C [45–50]. Additionally, the presence of voids seems to promote nucleation of sigma and chi phases due to segregation and/or other processes (partly unknown or different from past observations). This is a world-wide first-of-its-kind observation that was recently accomplished within the program [51].

2.5.2.2. Lot IV. The objective of the Lot IV campaign was the determination of basic properties for advanced EUROFER97 steels (i.e.,

Table 3
Preliminary trends for the DBTT of IGP tungsten.

Condition	DBTT, °C
Unirradiated	400
1 dpa / 400°C	1100
1 dpa / 600°C	≥1100
1 dpa / 800°C	1000–1025
1 dpa / 1000°C	≥1200

micro-alloyed EUROFER-type steels and/or thermo-mechanically heat treated) as a screening for down-selection. Since the irradiation hardening behavior of 9% Cr steels is well known, irradiation temperature and dose were set to 300°C and 2.5–3 dpa (Fe) respectively, to assess the candidate materials by means of tensile and toughness tests. The project included 10 different EUROFER97/2 and micro-alloyed EUROFER97 steel grades in various conditions as compiled in Table4 [52–54].

An overview of the selection relevant fracture mechanics test results is given in Fig.9.

Compared to the reference EUROFER97/2, most materials of the study proved to be softer, with drastically better ductility, both before and after irradiation [55]. Five grades proved to have better resistance against irradiation embrittlement, with a transition temperature shift ΔT_0 of about +50K after irradiation at 300°C, 3 dpa. For comparison: the expected shift for EUROFER97/2 is +110K. This successful reduction of DBTT shift was observed on EUROFER-like materials prepared as follows:

- Specific and optimized mechanical treatment with normalizing at 1250°C/1h and then rolling to a final rolling temperature of 850°C in 6 rolling steps with a reduction of 20–30% for each rolling pass (material J, or 'lab-cast EUROFER'). This material shows the best fracture toughness properties before and after irradiation of the tested materials, with a final transition temperature of −58°C.
- Reducing the amount of C & Mn, while increasing V & N, and applying a high-temperature tempering of 820°C (material H, I and P)
- Reduction of the amount of C and Ta, while increasing V and N, and specific ausforming process with 40% reduction ratio rolling at 650°C (material O)

A 'technological heat treatment' was applied on a EUROFER97/2 grade (material E), which led to the formation of a population of large carbides (> 1μm). Although no substantial difference was observed in the hardness or tensile properties compared to the rest of the tested materials, the fracture toughness was clearly degraded. These results give an approximation for what has to be expected with joints (i.e., heat treated beam welds) after irradiation.

Unfortunately, alloys M and N were exposed to a higher irradiation temperature >350°C. Therefore, it was not possible to draw any conclusion concerning the irradiation embrittlement and DBTT shift at the target temperature for these alloys. However, in terms of strength and hardness in the non-irradiated state, these materials exhibited similar mechanical properties compared to the EUROFER97 reference materials of the study (E, J).

Besides these dedicated low temperature materials, also two materials for high temperature applications were included in the campaign. Material L (EUROFER97/2) with an increased ultimate tensile strength by more than 200MPa and an improvement in creep lifetime by about 2 orders of magnitude compared to EUROFER97/2 exhibited a slightly better behavior than material E in terms of radiation-induced hardening and embrittlement, and retained significant ductility after irradiation.

Material K was produced via the same optimized thermomechanical treatment as material J, but from an altered composition with reduced

Table 4
Irradiated materials and material manufacturing conditions. AQ: air quenched; WQ: water quenched; AC: air cooled; LT: low temperature application; HT: high temperature application.

Code	Material type	Heat	Condition
E	EUROFER97/2	993,391	ferrite+980°C/0.5h+AQ+760°C+AC / reference chemical composition)
H	EUROFER-LT	J362A	1000°C/0.5h+WQ+820°C+AC / Modified C, Mn, V and N content.
I	EUROFER-LT	J363A	1000°C/0.5h+WQ+820°C+AC / Modified Mn, V and N content
P	EUROFER-LT	J361A	1000°C/0.5h+WQ+820°C+AC / Modified Mn and N content
J	EUROFER-LT	I196C	1250°C/1h and then rolling to a final rolling temperature of 850°C in 6 rolling steps with a reduction of 20–30% for each rolling pass, then AC
	Q&T: 880°C/0.5h+WQ+750°C/2h+AC / reference chemical composition		
K	EUROFER-HT	J427A	1250°C/1h and then rolling to a final rolling temperature of 850°C in 6 rolling steps with a reduction of 20–30% for each rolling pass, then AC
	Q&T: 1050°C/15min+WQ+675°C/1.5h/AC / Modified C, Cr and Mn content		
L	EUROFER97/2	994,578	1150°C/0.5h+AQ+700°C+AC / Modified Mn content
M	EUROFER97/2	993,391	1020°C/0.5h+AQ+1020°C/0.5h+AQ +760°C/1.5h+AC (double austenitization) / reference chemical composition
N	EUROFER-LT	VM2897	920°C/1.5h+AQ+920°C/1.5h+AQ+760°C/1h+AC (double austenitization) / Modified Mn, V and N content
O	EUROFER-LT	VM2991	1080°C/1h, cooling to 650°C and rolling, reduction 40% (from 30mm to 18mm)
	Tempering: 760°C/1h+AC / Modified C, V, N, Ta and Si content		

Mn and Cr content, and severely reduced C content. The material displayed a coarse microstructure and the irradiation induced in this material a strong increase of T_{0Q} (137°C), while its tensile properties at 300°C comprise high strength and yet relatively high uniform elongation (compared to other tested materials).

2.5.2.3. Lot IX. The objective of the Lot IX campaign was the provision of validation data for modeling irradiation effects, which requires a broader parameter field. Therefore, 4 temperatures between 600°C and 1200°C and 4 doses have been chosen for this task. The tests should deliver mechanical properties by micromechanics testing. The
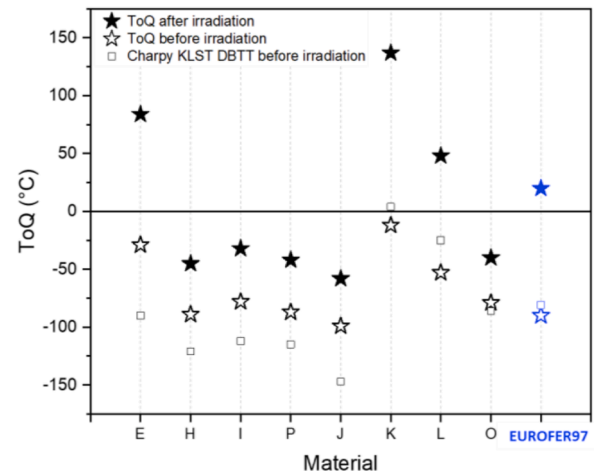

Fig. 9. T_{0Q} measurements by fracture toughness tests with the Master curve approach before and after irradiation at 300°C +/−30°C, 2.5 dpa. Materials M and N were excluded because of the failing irradiation temperature. Data of EUROFER97 (taken from MPH) are included as reference as well as DBTT measured by Charpy tests on unirradiated KLST samples.

irradiation focused on 3 tungsten materials: pure W (IGP), high purity single crystal W (110), ultra-fine grained W (PLANSEE 1mm sheet).

The mechanical properties of the irradiated tungsten grades were assessed by impulse excitation and depth-sensing indentation measurements. The values of Young's modulus, shear modulus and Poisson ratio are not affected by the irradiation. The mean hardness of the irradiated tungsten increases by 48, 45, 46, and 34% after irradiation at 600, 800, 900 and 1200°C, respectively [40,56-57].

Instrumented micro-hardness tests were performed, which delivered an overview on the influence of irradiation temperature and dose on hardness. Moreover, the same micro-test facilities were used to produce "creep" and "fatigue" data. In all cases, the results cannot easily be translated into or compared to available engineering data, since the definition of the material properties are quite different. Therefore, further analyses are required to assess the outcome and conclusions of this campaign [58,59].

2.5.2.4. Lot A. The objective of the Lot A campaign was the determination of tensile strength for an evaluation of advanced heat sink materials (screening for down-selection). The well-known irradiation softening behavior of CuCrZr was used as one selection criterion in the screening experiment, for which doses of about 2.5 dpa (Cu) or 1 dpa (W) were considered adequate to assess the candidate materials. The irradiation temperature range covers the temperature for water-cooling at ~150°C to 450°C as the new materials are supposed to extend the application temperature beyond those for CuCrZr at 350°C.

Five advanced heat sink materials in the as delivered condition were part of the campaign: CuCrZr-W(fiber) composite, CuCrZr-W(particle) composite, CuCrZr-W laminate, CuCrZrV (SAcwA), ODS Cu-Y$_2$O$_3$.

Based on the tensile test results [60], the tungsten-CuCrZr laminates and the CuCrZr-V alloys can be excluded (down-selected) from the future program, while the CuCrZr-W (particle) composites will be kept as back-up option. The best material appears to be CuCrZr-W(fiber) as the pseudo-ductility concept of this material seems to work and leads to both, high strength and good ductility even at 450°C. This is a considerable improvement over the baseline material CuCrZr. Not quite as good, but still promising are results for the commercial yttria-Cu ODS material. Since this irradiated heat was just a prototype – not optimized for divertor application – there seems to be a high potential for improvement. The LOT-A PIE campaign will be finalized in the course of 2021.

2.5.2.5. Lot B. The objective of the Lot B campaign is the determination of basic properties for an evaluation of baseline and advanced armor materials (screening for down-selection). Based on the knowledge from the Lot III campaign, namely that 1 dpa (W) is sufficient to cause significant irradiation hardening in tungsten and that irradiation hardening does not vary significantly between 400°C and 800°C, the number of irradiation temperatures were reduced to 600–800°C, 1000°C and 1100–1200°C. Static bending tests should provide data to characterize hardening and DBTT behavior.

Eight advanced armor materials were involved in the condition as delivered:

- W (ITER type, IGP)
- W (long fiber)-W composite
- W (short fiber)-W composite
- PIM W-Y$_2$O$_3$
- PIM W-TiC
- W-K doped plate 7mm (Tohoku Univ.)
- W3%*Re*-K doped plate 7mm (Tohoku Univ.)
- W-K doped plate 1mm (KIT/Plansee)

"Matchstick" (miniaturized 3P/4P bend bars) specimen geometry was used for all materials except the W(short fiber)-W and W(long fiber)-W materials, for which mini-Charpy (KLST) specimen geometry was used. In addition, pure W (IG-) was used as a reference to compare both geometries. All tests were performed in L-S orientation.
Fig.10

As can be seen in Fig.12, the potassium doped tungsten plate from Tohoku University performs best with respect to DBTT after irradiation at 600°C and 1100°C. In both cases, the DBTT shift is only about 250K. After the 1100°C irradiation only the K-doped W-*Re* alloy shows a similar low DBTT. Even the K-doped highly deformed tungsten sheet (KIT/Plansee) performed clearly worse in the bending tests, only slightly better compared to the reference tungsten (IGP). After irradiation at 600°C, all materials show a DBTT higher than 600°C, except for the K-doped Tohoku grade. Based on these results, both PIM tungsten heats will be excluded from the further WPMAT-HHFM R&D program (down-selection). The ongoing microstructure analyses will probably reveal more details about the fracture and embrittlement mechanisms.

The pseudo-ductility concept of the W(fiber)-W materials has been verified by 3 point bending tests as can be seen in Fig.11. Compared to the baseline (reference) material W (IGP), ductility in terms of uniform elongation is much lower in the unirradiated condition. After irradiation, however, there is an improvement, but only in total elongation. Therefore, it is difficult to assess a possible benefit or application for this material type.
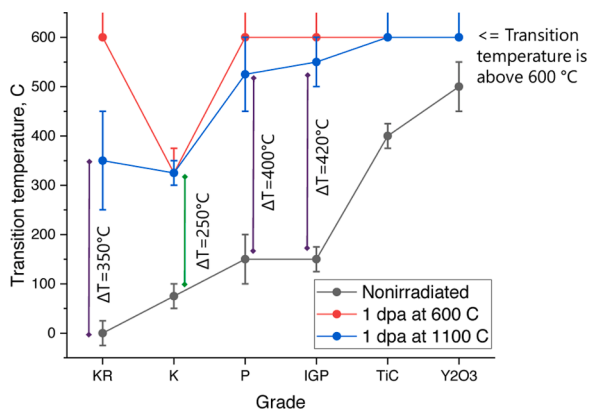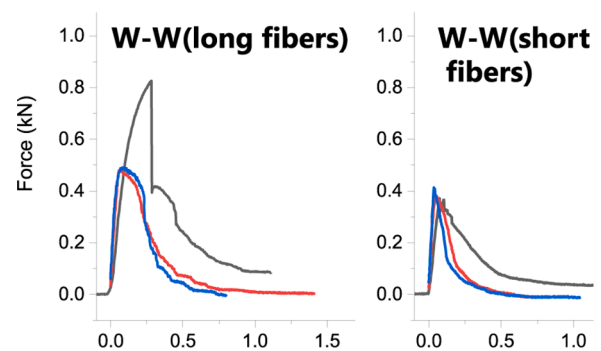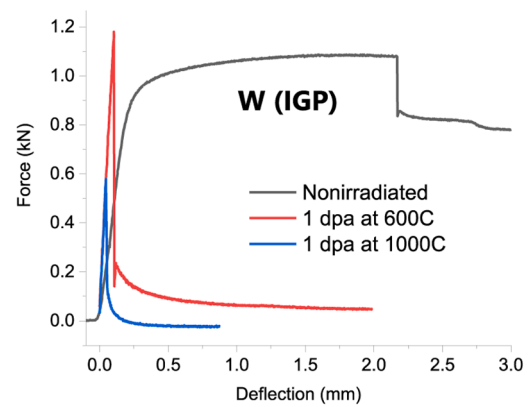

Fig. 11. Bending tests with the KLST specimens at 600°C for upper graph: W (IGP); lower graph: W-fiber W composites.

The reason for the improved "post-uniform elongation ductility" of the fiber material after irradiation to about 0.7–0.8 dpa at 1000°C is a high degree of ductile deformation of the fibers (the tungsten matrix is completely brittle). With these results, the focus in the future will be on the long fiber version showing better results with regard to pseudo-ductility.

2.6. Irradiation modeling

2.6.1. Objectives

Effort in materials modeling has been primarily focused on the development and application of multiscale models for simulating radiation-induced defect and dislocation microstructures of candidate fusion materials, with a renewed emphasis on linking atomistic simulations with the dislocation-based representation of microstructure and its evolution. Simulations, where appropriate, were compared with experimental observations of irradiated materials, including both ion- and neutron-irradiated materials data where in some cases quantitative agreement was established.

Applications of density functional theory continued providing significant and quantitatively accurate results. The problem of small spatial scale associated with density functional theory models has become apparent and requires making conceptual advances in the form of innovative mathematical algorithms. Kinetic Monte Carlo (kMC) methods show progress towards including elastic stress and strain effects in the simulations, but at the same time highlight the limitations associated with this simulation approach. The recognition of the part played by the internal degrees of freedom of defects, not yet included in kMC, but already included in stochastic dislocation dynamics, is expected to provide a foundation for further work and help overcome this significant difficulty in multi-scale simulations. Dislocation dynamics-based methods exhibited a notable progress, especially in relation to the treatment of stochastic and thermally activated processes, but the development of the dislocation-based simulation algorithms still require

Fig. 10. Overview on the DBTT and shift of DBTT. Code: KR=W-*Re*-K, K=W-K (Tohoku), P=W-K (KIT), IGP=W (Plansee), TiC=PIM W-TiC, Y$_2$O$_3$=PIM W-Y$_2$O$_3$. [60,61].

extensive and focused effort.

2.6.2. Achievements

Density functional theory calculations have now firmly established themselves as a reliable and accurate method for predicting energies and structures of radiation defects in materials [62]. This methodology has been extended to enable performing accurate calculations of relaxation volumes of defects. Relaxation volumes of defects determine the magnitude and anisotropy of lattice distortions, and hence are the quantities characterizing the strain that defects produce in a material exposed to irradiation. Relaxation volumes of defects have long been a subject of extensive experimental effort that revealed the challenges associated with attempts to measure the volume of a defect experimentally. The difficulties are partially due to the fact that self-interstitial atom defects diffuse rapidly in materials [63] or exhibit a tendency towards clustering [64]. Evaluating relaxation volumes from semi-empirical interatomic potentials is not reliable since the results are sensitive to the assumed many-body law of interaction between the atoms [65]. Still, knowing the volumes of defects is essential for modeling radiation effects on the macroscopic scale these volumes determine the magnitude of radiation-induced swelling or contraction [66] of materials, resulting from the accumulation of radiation defects.

Relaxation volumes of a vacancy and several high symmetry configurations of self-interstitial atom defects in some selected bcc metals, computed using density functional theory [67–69], are summarized in Table 5. The results are still sensitive to the choice of exchange-correlation functional, but the margin of error is very small in comparison with experimental measurements.

Density functional theory calculations have also been applied to the evaluation of relaxation volumes of defects in FeCr alloys [70]. The most significant new result in [68] concerns not the volumes of defects in the alloy, but rather the volumes of atoms forming the alloy itself. Calculations show that the volume of a substitutional Cr atom in bcc lattice Fe is 0.18 atomic volumes larger than the volume of a host Fe atom, defined as $a^3/2$, where a is the bcc lattice constant. At the same time, a substitutional Fe atom in bcc Cr is 0.05 atomic volumes smaller than that of the host lattice. This remarkable asymmetry, not compatible with Vegard's law [71] stems from the different magnetic structure of iron and chromium, where bcc Fe is ferromagnetic and bcc Cr is antiferromagnetic [72]. The significant difference between the volumes of Cr and Fe atoms in dilute FeCr alloys is responsible for the experimentally observed but still unexplained effects of radiation-induced Cr segregation [73,74].

Why is it significant for the assessment of the lifetime of materials in a fusion power plant? At relatively low operating temperatures, close to 300°C, radiation hardening and embrittlement of steels, containing 8% or more Cr, stems from the formation of Cr-rich α' precipitates [75]. The very small difference between the atomic volumes of Fe and Cr atoms in pure crystalline phases makes it hard to explain the observed accumulation of α' precipitates as a function of dose and account for the observed radiation embrittlement of steels. The unexpected finding that a Cr solute atom in Fe has a much larger relaxation volume than was expected from the established rules of formation of alloys, suggests that the effects of α' precipitation stems from the internal strain, which was never considered before in the treatment of precipitation.

Indeed, if a solute atom has a substantial relaxation volume, i.e. if its volume is significantly different from the atomic volume of the host material, it interacts with the local stress via the term $E=p\Omega$, where $p=-(1/3)\sigma_{kk}$ is the hydrostatic pressure, and Ω is the relaxation volume. It is this interaction that drives the decomposition of alloys, containing oversized solute atoms, under irradiation.

Going up the length scales and recognizing the significance of lattice distortions generated by the defects, which can now be accurately modelled using density functional theory, we pose the question about the microstructure that such distortions produce in the limit of high dose.

The difficulty associated with high dose simulations is often not appreciated. For example, even a large-scale simulation of a collision cascade, initiated by a high energy neutron impact [76], in fact corresponds to a small irradiation exposure of 10^{-4} dpa. To show this, it is sufficient to note that in a simulation of a cascade it is necessary to disperse the initial recoil energy between the atoms in a simulation cell. Hence the number of atoms in the cell must be at least as large as $N_{cell}=E_{recoil}/E_{th}$, where E_{th} is the thermal energy ~ 0.01eV. Since the number of defects that a collision cascade with energy E_{recoil} is going to produce, equals $N_d=E_{recoil}/2E_0$, where E_0 is the threshold energy for the generation of a Frenkel pair of a vacancy-self-interstitial atom defects. Taking $E_0 \sim 50$eV, we find that the irradiation dose that a single collision cascade produces does not exceed $N_d/N_{cell}=E_{th}/E_0=0.01\text{eV}/(2\times50\text{eV})=10^{-4}$ dpa.

This agrees with direct simulations of cascade events, showing that even several thousand successive high energy cascade simulations produce radiation exposure of several tenths of a dpa [77,78]. Since in applications the dose may approach tens or even a hundred dpa [79], it is necessary to develop computational algorithms capable of generating high dose microstructure at a reasonable expenditure of supercomputer time. The Creation-Relaxation Algorithm (CRA) developed in [80] has enabled performing such simulations. High dose defect and dislocation structures formed at high dose, approaching 20 dpa, have now been simulated on a million-atom scale [63,76].

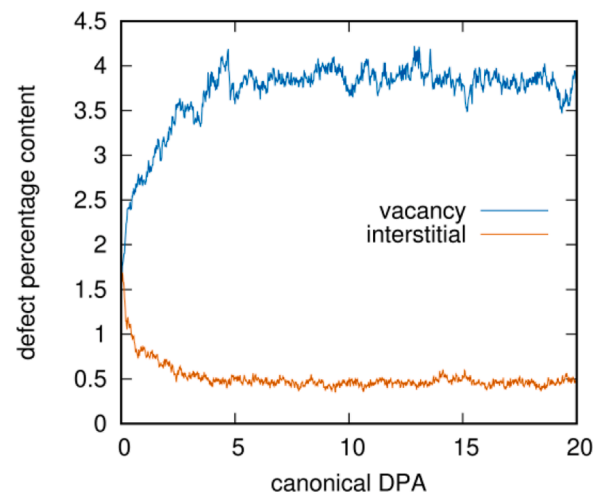Fig.12 illustrates an application of the algorithm to the simulation of

Table 5
Relaxation volumes of a vacancy and various high-symmetry self-interstitial atom defects in selected body centered cubic metals, computed using density functional theory and the GGA-PBE exchange-correlation functional [67]. Relaxation volumes of defects are given in atomic units $\Omega_0=a^3/2$, where a is the bcc lattice parameter. The volume of a 111 self-interstitial atom defect is the average between a crowdion and a dumbbell configuration. For the relaxation volumes of defects in fcc metals see Ref. [68].

Element	vacancy	111	110	tetra	100	octa
V	−0.35	1.47	1.47	1.50	1.53	1.65
Nb	−0.45	1.55	1.54	1.57	1.65	1.65
Ta	−0.45	1.52	1.50	1.56	1.64	1.65
Cr	−0.41	1.37	1.43	1.61	1.61	1.61
Mo	−0.37	1.54	1.58	1.62	1.68	1.68
W	−0.32	1.71	1.75	1.79	1.87	1.87
Fe	−0.22	1.66	1.62	1.62	1.86	1.85

Fig. 12. Isolated (non-clustered) defect content in bcc Fe plotted as a function of dose, measured as canonical displacement per atom (cdpa). These high dose simulations suggest that while the onset of the asymptotic microstructural dynamic steady state occurs at the dose close to 2.5 cdpa, the ultimate steady state microstructure develops at a somewhat higher dose close to 5 cdpa, in agreement with experimental observations [74].

a high dose microstructure in bcc Fe. As a function of dose, microstructural evolution proceeds in several stages. Up to the dose of ~0.05 dpa, corresponding to the typical end of life exposure of a pressure vessel in a fission reactor [81], radiation damage accumulates linearly with dose. Above 0.05 dpa, the accumulation of damage is non-linear, and this agrees with experimental observations showing that physical and mechanical properties characterizing high dose microstructures either saturate [82] or exhibit runaway behavior [83]. The simulations below refer to the lower-temperature mode of accumulation of damage, where properties saturate with dose. Models for the high temperature evolution of steels, corresponding to the operating temperatures between 350°C to 550°C, are under development.

Figs.12 and 13 show that a material irradiated to high dose at a relatively low temperature, transforms into a quasi-steady microstructural state. This state is characterized by a high average concentration of defects, where self-interstitial defects coalesce into dislocation loops and dislocation network, whereas vacancies remain dispersed in the microstructure. The simulations explain the unusually high vacancy content found in ferritic-martensitic steels exposed to irradiation below ~300°C [84], an effect that has long eluded explanation but is critical to understanding the saturation of mechanical and physical properties of steels exposed to high irradiation dose [82]. The high vacancy content also accounts for the high hydrogen isotope retention in irradiated materials, where estimates derived from the simulations and experimental observations suggest that hydrogen retention in highly irradiated materials can approach 1 at%.

The high dose microstructure predicted by CRA simulations typically contain ~1% of vacancies. While the occurrence of saturation and the variation of microstructure as a function of dose agree with experimental observations [66,87], direct simulations of collision cascades shown in Fig.14 suggest that the local heating generated by the cascades reduces the number of defects in comparison with CRA predictions. A combination of CRA and cascade simulations enables generating fully converged high dose microstructures in a computationally efficient manner [88]. The predicted vacancy content in the high dose limit agrees well with experimental observations [84], showing that the microstructure illustrated in Fig.13 is representative of that of steels exposed to high irradiation dose at a temperature below ~300°C.

Since the accumulation of internal volumetric strain in materials, resulting from the accumulation of defects, is responsible for the dimensional changes and swelling, it is essential to be able to perform quantitative measurements of swelling, even if its magnitude is
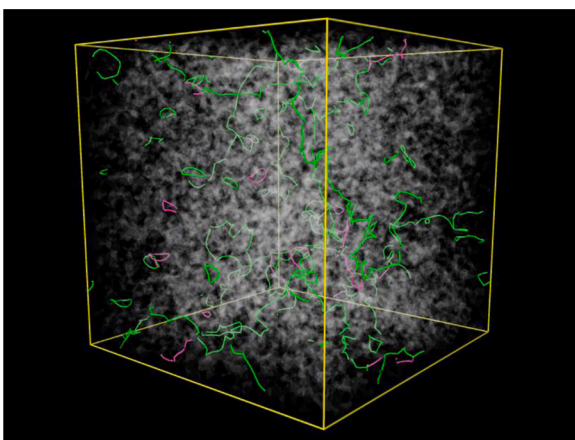

Fig. 14. Number of vacancies as a function of dose/the number of cascade events in a simulation cell, simulated using sequential generation of collision cascades in FeCr alloys containing different amounts of Cr [62]. Simulations were performed using cells containing ~500,000 atoms. 1000 vacancies correspond to the asymptotic high-dose vacancy content of approximately 0.2%.

relatively low. Indeed, in a reactor component exposed to irradiation, where the magnitude of swelling is ω, the internal stresses that develop in response to irradiated-driven deformations are on the order of $\mu\omega$, where μ is the shear modulus of the material [89,90]. Since for tungsten and steels μ approaches a hundred GPa, even a small amount of swelling is expected to generate high internal stresses in irradiated reactor components – which subsequently evolve by radiation-driven stress relaxation, see below. For the purpose of estimating the magnitude of radiation-induced stress, microscopic modeling is linked with finite element model (FEM) simulations. While predictions require extensive experimental validation and analysis, particularly in the range of high operating temperatures, the new findings highlight a general point significant in the context of the assessment of the lifetime of reactor components exposed to irradiation. Since the characteristic attenuation distance of neutrons in a steel component is ~30cm [91,92] and is comparable with the size of the component itself, the accumulation of defects is expected to produce swelling that is spatially heterogeneous. The magnitude of strains and stresses resulting from the gradient of swelling can be estimated numerically for simplified geometries of components. An example of such analysis is shown in Fig.15, where radiation-induced elastic stresses are evaluated for a model blanket module structure exposed to a spatially varying field of neutron irradiation [90]. The origin of dimensional changes, responsible for the stress, is similar to that in fission fuel cladding, where the level of radiation exposure is similar to that expected in fusion. While the gradient of neutron flux in fission cladding is small, deformations are caused by the crystal anisotropy and texture of the cladding material [93]. In fusion, stress and deformation result from the spatial heterogeneity of neutron exposure.

Quantitative determination of swelling in the limit where the runaway evolution [83] has not yet occurred and swelling is still relatively small, below 1%, is a challenging experimental task [82]. Observing swelling in a transmission electron microscope (TEM) normally involves analysing the void microstructure and evaluating the total volume of cavities in a unit volume of an irradiated material. Since the small vacancy clusters, forming at relatively low temperatures or at a low dose, are difficult to resolve in TEM, the data shown in Fig.16 used

Fig. 13. A view of the microstructure of bcc iron exposed to the irradiation dose of 2.5 dpa. Most of self-interstitial atoms have coalesced into dislocation loops and dislocation network, while vacancies remain dispersed in the bulk of the material. The high vacancy content predicted by the simulations agrees with positron annihilation spectroscopy (PAS) experiments [84] as well as with the variation of hydrogen isotope retention as a function of dose [85,86].
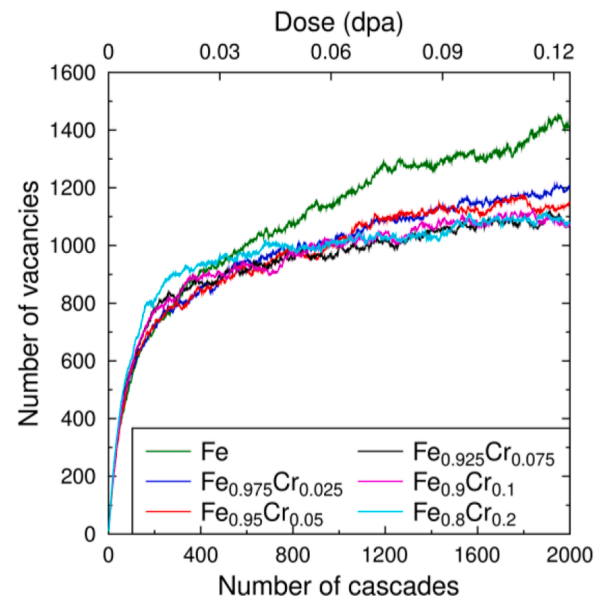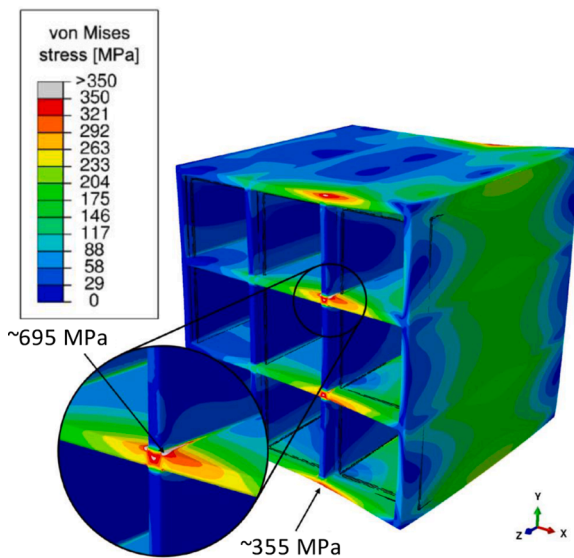
Fig. 15. Spatially varying exposure of materials to irradiation, resulting from the attenuation of the neutron flux in the component structure, gives rise to stress and distortions in a breeding blanket module, which is modelled assuming to be free from external geometric constraints and external load. The local von Mises stress is found to be maximum at a junction between the internal walls of the module [81].
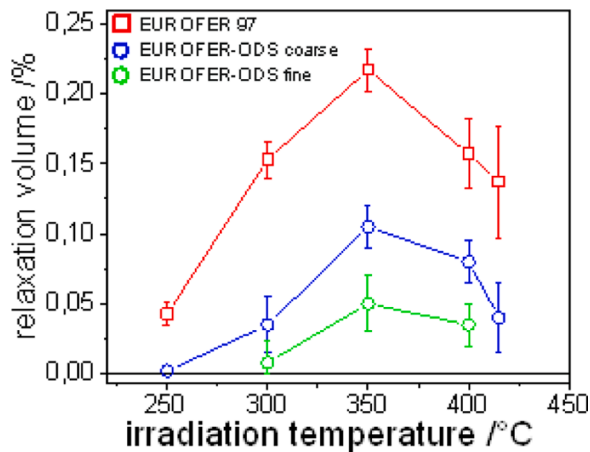

Fig. 16. Swelling of ferritic-martensitic steel EUROFER97 and two varieties of ODS steels based on EUROFER 97 exposed to 16.3 dpa and shown as a function of temperature, measured using electron microscope observations of dislocation loops.

an alternative experimental approach, involving the assessment of the total *volume of dislocation loops* [94]. The volume of a dislocation loop equals the scalar product of the Burgers vector of a loop and its vector area [95], namely $V=(\boldsymbol{b}\cdot\boldsymbol{A})$. The assessment of swelling using this formula is more accurate in the limit where the absolute value of swelling is low, below 1%. The temperature variation of swelling shown in Fig.16 correlates well with other experiments [96] and provides a first quantitative example of observation of radiation-induced swelling in fusion steels.

Radiation-induced volumetric swelling is one of the effects of internal strain and deformation resulting from exposure to irradiation. If the irradiated material is constrained, like it is under ion irradiation conditions, where a thin layer of material exposed to irradiation is constrained by the substrate, microstructural evolution exhibits a more complex pattern of radiation-induced deformation than a directionally isotropic volumetric swelling.

Fig.17 shows that in tungsten exposed to ion irradiation, the lattice strain measured in the direction normal to the surface, initially increases linearly as a function of irradiation dose, but then changes sign as the irradiation exposure approaches ~0.1 dpa, becoming negative at higher irradiation dose. The phenomenon is predicted by the high dose microstructural simulations [66,82] and is an example illustrating the effect of irradiation-induced stress on the evolution of microstructure. This highlights the strongly non-linear nature of microstructural evolution of materials in the high dose limit and in the presence of external geometrical constraints or applied stress and is also a striking case illustrating the radiation-induced stress relaxation [97]. The analysis performed in [66] shows that a combination of stress, including the self-stress from dimensional changes and swelling, and *high-dose* irradiation, together produce irreversible dimensional changes in a component exposed simultaneously to mechanical load and irradiation.

Concluding this section, we note the effect of radiation exposure on thermal conductivity of irradiated metals and alloys [98]. The effect of defects on thermal conductivity can be estimated using density functional theory calculations and Boltzmann transport theory analysis. It is possible to estimate the effect of accumulation of defects on the thermal conductivity of tungsten that according to Fig.18 is highly sensitive not only to the content of defects but also to temperature.
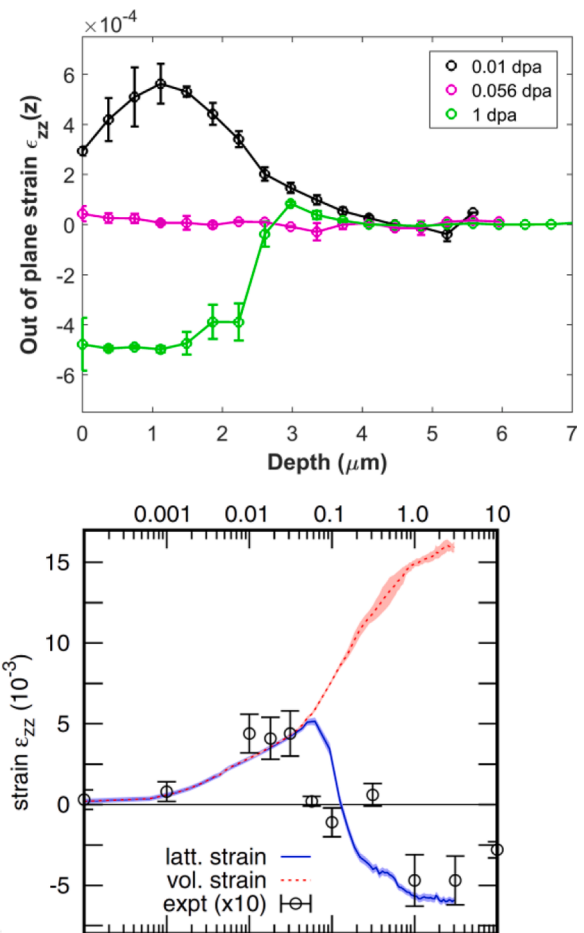

Fig. 17. (Top) Depth-resolved strain in tungsten irradiated with 20 MeV self-ions, measured using diffracted X-ray intensity of the [008] Bragg peak for three values of radiation exposure. The fact that the observed strain changes sign from positive at low dose to negative at high dose is an example of irreversible radiation-driven structural and stress relaxation [66]. (Bottom) Experimentally observed strain plotted as a function of dose, compared with atomistic simulations performed using the Creation-Relaxation Algorithm. The observed non-linear variation of strain results from the combined effect of defect-induced stress and stress relaxation, also driven by irradiation.
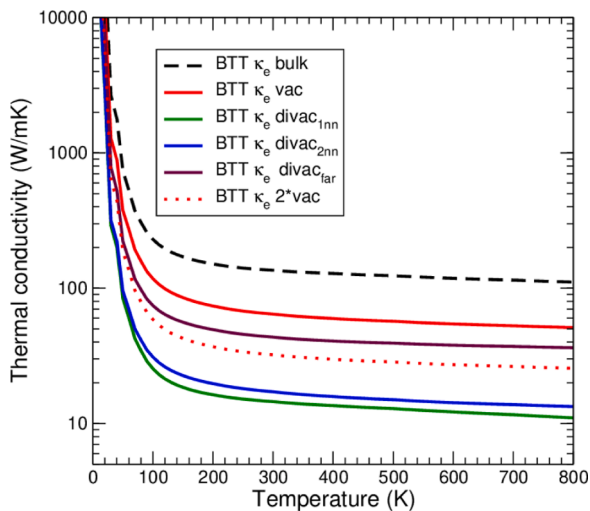
Fig. 18. Thermal conductivity of tungsten computed as a function of temperature for two values of vacancy content. Bulk thermal conductivity, plotted as a function of temperature, is included as a reference. Calculations were performed using a 128-atom cell, and hence the single vacancy curve (red) corresponds to the vacancy content of 0.7%, whereas the divacancy curve corresponds to 1.4% vacancies per lattice site. These concentrations of defects are high (this stems from the limitations on the size of the simulation cell), explaining why the effect of defects on thermal conductivity is significant.

Summarizing the results described in this section, we note that the development of multiscale microstructural models for irradiated materials has for the first time enabled direct simulations of microstructure of materials exposed to high irradiation dose, illustrated in Fig.13. It shows a microstructural asymmetry where vacancies form finely dispersed dense atmosphere but self-interstitial defects form dislocation loops and extended dislocation networks. The spatially heterogeneous exposure to irradiation results in the anisotropic accumulation of local internal excess volume, resulting in swelling, dimensional changes, and non-linear stress/strain relaxation. In the high dose limit, the evolution is strongly non-linear, illustrated by modeling where predictions agree with observations shown in Fig.17.

The microscopic models for defects can now be linked to macroscopic finite element treatment that is expected to enable the analysis of dimensional changes, driven by the combined effects of applied and internal radiation-induced stresses and radiation-stimulated stress/strain relaxation.

We highlight the role of radiation-driven stress relaxation, a phenomenon that has so far received little attention, but now emerges as one of potentially critical aspects of behavior of materials operating under a combination of loading conditions and high irradiation dose. The complex non-linear nature of the phenomenon, involving a combined *in-situ* action of stress and irradiation, has now been recognized [66].

3. Outlook

The main objectives for future work include extension of engineering data base for the three baseline materials EUROFER97, tungsten and CuCrZr, i.e. closing gaps in the material property handbook and reducing uncertainties in performance window elaborated based on the results of neutron irradiation campaigns. This requires various irradiation campaigns in MTRs up to neutron fluence representative for DEMO, i.e. 20–50 dpa for the structural material of the First Wall. Accompanying programs with multi-ion beam irradiation and irradiation modeling are mandatory to extend the knowledge in microstructural changes particular to fusion environment and based thereon predict not or not yet accessible material properties in a high dose neutron

environment also as a function of the operational stress and temperature fields and to reduce uncertainties inherent due to different neutron spectra.

PIE results on advanced steels and high heat flux materials from campaigns underway will allow selection of a few options for risk mitigation to be investigated in parallel to baseline materials. Thereby, increased efforts towards technology are needed, i.e. the candidate materials, both baseline and risk-mitigation options have to be industrially manufactured in larger batches and characterized as well as bulk or joint material and in combination with functional materials like barriers and coatings.

The development of DDC and design methodologies for in-vessel components are essential for the evaluation and selection of engineering options and mandatory input for preliminary safety analyses (precursor to any nuclear licensing process). The validation of the newly developed design rules also needs strong support from verification experiments and simulations applying multi-physics and irradiation modeling.

The work plan follows the recommendations of the Gate Review process.

3.1. Engineering data and design integration

The development of MPH chapters for baseline materials must be pursued, closing gaps in material properties and providing engineering data as well as input to appendices in design codes. The priorities are to provide data for properties in the irradiated condition as well as properties for similar and dissimilar joints. During this time the DDC shall evolve to become, at the end of Conceptual Design Phase, the single entry point for structural design analysis of all in-vessel components. To achieve this objective, the links with existing (nuclear) C&S (Codes & Standards) must be strengthened and validation of new and extended fusion application related design rules must progress in parallel. This shall be supported by an extensive in-house testing program geared also towards the definition of a set of guidelines for small specimen test techniques (SSTT) of irradiated specimens as basis for the definition of a standard of "fusion specific SSTT". Dedicated updates of MPH and DDC for down-selection of engineering options are planned in 2023 and 2026 aligned with the actual planning of the DEMO Gate Review process (Gates G2 and G3) [99]. The final goal is to provide guidance to the design process.

3.2. Advanced steels

The objective is to select the most promising steel batches and associated thermomechanical treatments to be fabricated at larger scale (typically a few tons) and subjected to a comprehensive mechanical test program in the relevant temperature range (RT-700°C), supplemented by joining studies. The selection criteria, to be applied to the various steel heats and treatments investigated up-to-date, can be summarized as follows: steels for high temperature application should have mechanical strength and thermal creep resistance compatible with operation up to about 650°C while retaining impact and toughness properties close to those of EUROFER. Regarding steels for low temperature applications, the irradiation behavior is of course the key issue. Following 2.5 dpa irradiation at 300°C in HFIR, compared to EUROFER in the reference metallurgical condition, several experimental materials/treatments exhibited lower irradiation-induced embrittlement. In particular specific thermomechanical treatments applied on EUROFER were shown to be beneficial. However additional data at higher dpa is needed to confirm these first results and allow a selection of the most suitable candidate materials, which should be performed in a first step end of 2024 and a final selection of the risk mitigation material for the engineering design will be done end of 2027. Finally, ODS steels are arguably the most promising materials for first wall application, including for water cooled reactor concepts, due to their outstanding

irradiation tolerance, especially regarding helium-induced embrittlement, combined with very high tensile, fatigue and creep strengths over a wide temperature range. Fully ferritic ODS (typically with 14%Cr) have the highest mechanical strength values, however tempered martensitic ODS or duplex ferritic-martensitic steels (Cr content in the 9–12% range) have better workability and tend to have more isotropic microstructures and properties. The objective during in the Conceptual Design Phase is first to select ODS grades with the best balance of properties for first wall application. The nano-oxide type, coherency with the matrix, size distributions and number densities will be investigated in detail since they are key for the irradiation resistance and helium management characteristics. In parallel, the fabrication route, i. e. mechanical alloying of powders, will be optimized in view of industrial large scale production (selection of milling method and parameters, use of elemental powders or pre-alloyed powders etc.).

3.3. High heat flux materials

Similar to the objectives for advanced steels, the objective is to select the most promising plasma facing and heat sink materials as well as the correlated manufacturing options. In contrast to advanced steels, for the heat sink materials in the divertor and in particular the strike-point region a first selection has already taken place based on the available irradiation screening results limiting the options to W-fiber reinforced Cu-based materials, ODS-Cu alloys using Y_2O_3 instead of Al_2O_3 and keeping the W-particle reinforced Cu-based alloy as back-up option. All these materials require further development on the industrial scale, the manufacturing of semi-finished products, i.e. pipes, correlated to the selected divertor design(s) and the subsequent material characterization and qualification. In particular for the fiber reinforced composites providing a specific and optimized microstructural set-up optimized for the pipe geometry, a dedicated development of characterization methods needs to be performed that can be applied before and after irradiation. The same applies for the characterization of material joints characteristic for the divertor monoblock configuration to finally allow a design by analysis in contrast to the actually followed strategy of a design by experiment.

As plasma facing materials for the first wall and potentially also for the lower loaded parts of the divertor the industrial upscaling of self-passivating tungsten alloys is one high priority task as the material yet is the only option to deal with the risks associated with a LOCA. This development is strongly related to the large scale fabrication of high quality and also economically viable mechanically alloyed powders. While this clearly determines the scope for the lower loaded parts in a fusion reactor, the material development for the strike point region is less straight forward. Based on recent assessments by the divertor design group on monoblock mock-ups representing the favored divertor design, at least in the non-irradiated case industrially available pure tungsten in the as received and aged / recrystallized condition has performed well under fatigue (20 MW/m^2) and overload (25 MW/m^2) tests [8]. Accordingly, the main focus now would be on providing relevant data for pure W materials after neutron irradiation including the before mentioned characterization of joints. Nevertheless, as this is still correlated with a certain risk, the development and characterization of a very limited number of materials will continue, focusing mainly on K-doped tungsten materials and dedicated fabrication technologies. Nevertheless, the combination of different materials suited either for the low temperature range by providing improved fracture properties, e.g. W-fiber reinforced W, or for the high temperature range providing high thermal stability and fatigue resistance, e.g. particle reinforced W, will still be kept as back-up options. The same applies for alternative manufacturing technologies like additive manufacturing of plasma and heat sink materials via laser or electron beam melting, which would provide a higher flexibility in the component design if this turns out to be required in the course of the Conceptual Design Phase.

In both cases, plasma facing and heat sink materials, the set

milestones are identical to those for advanced steels, i.e. a first selection at the end of 2024 and a final selection for the engineering design phase end of 2027, driven by the need to obtain further data on industrially produced products and technological specimens in particular after irradiation.

3.4. Functional materials

The use and selection of optical and dielectric materials for DEMO is strongly related to finally used technologies, in particular in the field of diagnostics. However, as long as those diagnostics have not been clearly identified, the only option is to base further investigation on an extrapolation of existing technologies to the DEMO-relevant environment. As suitable and industrially available window materials for application in the optical and infra-red range have been identified, providing high optical transmission also after neutron and gamma irradiation, the main aim will be to provide further design input, i.e. additional material properties for implementation into window components including information on suitable joining technologies. Depending on the final positioning of these windows determining the operationally expected dose and temperature, further investigations towards higher dose levels > 1 dpa and/or a wider range of temperatures need to be performed. Alternatively, the application of mirrors and the degradation of reflectivity, mostly depending on the interaction with plasma species and only to a minor extent on other kinds of irradiation damage, require even more attention than they get at the moment.

In contrast to optical materials, dielectric materials used in various kind of diagnostics but also as insulators in the divertor and breeding blanket components still require further analyses. One reason is that the occurring damage in these materials seem to follow a non-linear relationship with the absorbed irradiation dose showing the highest damage at very low damage levels. This requires further assessment to understand the influence of this non-linear change in material properties on the performance of the individual diagnostic. In addition, limitations in material characterization techniques require the application of comparably large specimens which are difficult to implement in standard irradiation channels in MTRs to obtain not only qualitative but also quantitatively robust material data.

3.5. Irradiation

Irradiation campaigns are planned in European MTRs in Belgium, Hungary. The tests should focus on further screening campaigns of advanced structural and high heat flux materials, the determination of handbook data for functional materials as well as specialized requests for breeding blanket and divertor applications, e.g. dissimilar joints. Another focus will be on the delivery of data base and materials handbook data for the whole operational temperature range covering both breeding blanket and divertor applications. In this regard, the planning for three further irradiation campaigns (one in the Russian BOR-60 and two in the US HFIR reactor) was done and implementation is ongoing.

According to plan, the BOR60/RIAR campaign will address gaps in the EUROFER97 database at high dose that is at the moment not accessible in a short time frame in European MTRs: (1) irradiation creep behavior, (2) fracture mechanics data, (3) high temperature irradiation effects, (4) weld degradation, (5) neutron doses equivalent to both a starter blanket and a blanket for phase 2 (20–50 dpa), and (6) macroscopic swelling experiments. The irradiation will be executed in several stages and capsules, which are subdivided to provide two irradiation temperatures (330°C and 550°C) and two dose levels (20 dpa and as high as possible within the remaining reactor lifetime). The material properties (tensile, Charpy, R-curve/J-integral, LCF, in-pile-creep, volumetric swelling, hardness) will be determined for EUROFER97/3 in two different heat treatment conditions (optimized for low- and high-temperature operation).

The irradiation in HFIR/ORNL comprises: (1) Tensile, fracture

toughness, hardness, thermal conductivity, and microstructure analyses on EUROFER97/2 in a simulated technological condition (similar to beam weld microstructure) with a neutron dose of 20 dpa for irradiation temperatures of 220°C, 250°C, 300°C, and 350°C by 2023. (2) The determination of the impact of transmutation He gas generation on neutron irradiation damage in 9%Cr steels using isotopic tailoring approaches. It includes (a) the extension of an ongoing irradiation of ^{54}Fe-EUROFER to ~25–30 dpa for the sake of generating high dose data at temperatures of 300, 385 and 525°C, (b) neutron irradiation to approximate target dose levels of 12–15, and >50 dpa at ~300, 400 and 500°C for ^{54}Fe and $^{58/60}$Ni isotopically tailored EUROFER-type materials (c) PIE of the isotopically tailored materials. The estimated performance period is about 52 months.

In the frame of all these irradiation campaigns, an additional focus will be given to the evaluation of the materials microstructure to tackle the needs of the modeling program allowing extraction of data as well as benchmarking of material models.

3.6. Test blanket module (TBM)

Work is also planned, in collaboration with Fusion for Energy, on the qualification of EUROFER97 as structural material for the European TBMs in ITER. It is recalled that the TBMs are considered as nuclear pressure devices according to French regulation and the code selected for their design and fabrication is RCC-MRx. This implies launching an extensive characterization program for the base material in non-irradiated and irradiated (up to 3 dpa at multiple irradiation temperatures) conditions, as well as qualification of the corresponding welded joints and associated design rules. The final objective is to produce an updated version of the EUROFER Material Data File for RCC-MRx before 2025, the date set for the final design review of the TBMs. At the same time, this will provide valuable feedback for the main WPMAT program on the requirement for codification in nuclear C&S, as well as design data for non-irradiated and low-irradiated EUROFER structures, as not all components in DEMO will be exposed to the maximum neutron fluence. The acquired information will feed in to the development of the EUROFER MPH and DDC-IC.

3.7. Materials technology development

As part of the materials design interface, dealing with technological issues for the design that are clearly related to materials, dedicated programs are set-up to deal with three main concerns:

- Large scale manufacturing of EUROFER97 (>>10 t) and alternative risk mitigation materials suitable for the needs of DEMO and therefore going beyond the fabrication of material batches ordered in the frame of the ITER TBM program. The focus should be on composition, microstructure, properties, alternatives to established production routes and applicability of thermo-mechanical treatments.
- Assessment of welding techniques foreseen to be used for the fabrication of the breeding blanket focusing on defining and setting-up specifications and guidelines, evaluation of material properties and modifications and correlated impact on design.
- Assessment of effect of coating techniques for functional coatings (e. g. corrosion and permeation) on materials and vice versa as a function of the operational conditions by dedicated testing (mechanical, aging, etc.).

3.8. Modeling

The development of models linking the microscopic effects of accumulation of defects with macroscopic FEM analysis for computing macroscopic operational parameters, strain, stress, temperature, local magnetic properties etc., enabling the treatment of self-consistent non-linear coupling of these parameters, is the next step in the evolution of multiscale materials modeling, linking it to advanced computing and engineering.

The microscopic phenomena that are expected to be affected by the spatially varying stress, strain and temperature are the accumulation of transmutation gas elements, helium and hydrogen isotopes, including tritium. Future research is also expected to involve modeling microstructurally complex materials showing better stability under irradiation in the high dose limit. Models will be developed to simulate local and global responses of components to stress-driven and radiation-driven plasticity and deformation, and effects of segregation of alloying elements as well as transmutation products, to assess the effect of segregation and phase transformations on the mechanical and thermal properties of materials under realistic operating conditions.

Within the framework of this particular development route, the first aim is the development of a component-level Virtual Tokamak Reactor (VTR) model, for the specific purpose of predicting the distribution of strains and stresses generated by the combined effects of external loads (gravitational, magnetic, and resulting from irradiation), and the radiation and thermal stress relaxation effects, by 2024. Including crystal plasticity effects and crystal plasticity treatment of embrittlement will be the following step expected 2026, and from then a plastic model for VTR components including radiation and thermal plastic deformation and creep is expected for 2027.

3.9. International collaboration

After the successful outcome of the first Broader Approach agreement between EU and Japan, which lasted from 2007 to 2017, a new agreement was signed in 2020 for the implementation of the "Phase II" activities, which will last until 2025. In this renewed collaborative framework, further work is planned for the development and characterization of materials and corresponding design criteria for the DEMO In-Vessel components. The work-program was defined to benefit from the complementarity of the R&D planned by both parties. Common MPHs will be developed for baseline materials. Different types of W and CuCrZr alloys (different manufacturers, different production processes, different heat treatments) will be characterized in parallel to cover the inherent material scatter and speed up the definition of common procurement specifications. Common SSTT will be developed towards optimization of neutron fusion sources. Joint work on DDC will benefit from the deterministic design approaches mostly followed in EU and the probabilistic approaches investigated by Japan. Finally, common R&D on modeling of fusion neutron effects will allow for a better understanding of underlying physics phenomena involved in embrittlement and swelling of materials.

Acknowledgments

References

[1] T. Donné, W. Morris, European Research Roadmap to the Reaslisation of Fusion Energy, EUROfusion (September 2018).

[2] M. Rieth, et al., Review on the EFDA programme on tungsten materials technology and science, J. Nucl. Mater. 417 (2011) 463–467.

[3] M. Porton, et al., Structural integrity for DEMO: an opportunity to close the gap from materials science to engineering needs, Fusion Eng. Des. 109 (2016) 1247–1255.

[4] M. Gorley, et al., Materials engineering and design for fusion - Towards DEMO design criteria, Fusion Eng. Des. 136 (2018) 298–303.

[5] E. Gaganidze, et al., Development of EUROFER97 database and material property handbook, Fusion Eng. Des. 135 (2018) 9–14.

[6] G. Pintsuk, et al., Recrystallization and composition dependent thermal fatigue response of different tungsten grades, Int. J. Refract. Metals Hard. Mater. (2018) 97–103.

[7] Ch. Linsmeier, et al., Development of advanced high heat flux and plasma-facing materials, Nucl. Fusion 57/9 (2017), 092007.

[8] J.-.H. You, et al., High-heat-flux technologies for the European demo divertor targets: state-of-the-art and a review of the latest testing campaigns, J. Nucl. Mater. 544 (2021), 152670.

[9] M. Richardson, et al., Technology readiness assessment of materials for DEMO in-vessel applications, J. Nucl. Mater. 550 (2021), 152906.

[10] G. Federici, et al., An Overview of the EU breeding blanket strategy as integral part of the DEMO design effort, Fusion Eng. Des. 141 (2019) 30–42.

[11] D. Stork, et al., Developing structural, high-heat flux and plasma facing materials for a near-term DEMO fusion power plant: the EU assessment, J. Nucl. Mater. 455 (2014) 277–291.

[12] L. Pilloni, et al., Nucl. Mater. Energy 17 (8) (2018) 129–136.

[13] L. Pilloni, et al., Nucl. Mater. Energy 19 (2019) 79–86. I.

[14] M. Rieth, et al., Technological aspects in blanket design: effects of micro-alloying and thermo-mechanical treatments of EUROFER97 type steels after neutron irradiation, Fusion Eng. Des. 168 (2021), 112645.

[15] A. Puype, et al., J. Nucl. Mater. 494 (2017) 1–9.

[16] F. Dalle etal., Development of boron-added 9Cr RAFM steels with enhanced creep lifetime, to be submitted to Proceedings of ICFRM 20.

[17] M. Rieth, et al., Impact of materials technology on the breeding blanket design - Recent progress and case studies in materials technology, Fusion Eng. Des. 166 (2021) 112275.

[18] D. Pazos, et al., ODS ferritic steels obtained from gas atomized powders through the STARS processing route: reactive synthesis as an alternative to mechanical alloying, Nucl. Mater. Energy 17 (2018) 1–8.

[19] G. Pintsuk, Tungsten As a Plasma-Facing Material, 4, Elsevier Inc., 2012.

[20] S. Noce, et al., Nuclear analyses for the design of the ITER-like plasma facing components vertical targets of the DEMO divertor, Fusion Eng. Des. 155 (2020), 111730.

[21] J.-.H. You, A review on two previous divertor target concepts for DEMO: mutual impact between structural design requirements and materials performance, Nucl. Fusion 55 (2015) 113026.

[22] A. Durif, et al., Impact of tungsten recrystallization on ITER-like components for lifetime estimation, Fusion Eng. Des. 138 (2019) 247–253.

[23] M. Rieth, et al., Recent progress in research on tungsten materials for nuclear fusion applications in Europe, J. Nucl. Mater. (2013) 482–500.

[24] S. Antusch, et al., Processing of complex near-net-shaped tungsten parts by PIM, Nucl. Mater. Energy 16 (2018) 71–75.

[25] R. Neu, et al., Tungsten fibre-reinforced composites for advanced plasma facing components, Nucl. Mater. Energy 12 (2017) 1308–1313.

[26] J.W. Coenen, et al., Advanced materials for a damage resilient divertor concept for DEMO: powder-metallurgical tungsten-fibre reinforced tungsten, Fusion Eng. Des. 124 (2017) 964–968.

[27] Y. Mao, et al., Design of tungsten fiber-reinforced tungsten composites with porous matrix, Mater. Sci. Eng.: A 817 (2021), 141361.

[28] J. Reiser, et al., Ductilisation of tungsten (W): tungsten laminated composites, Int. J. Refract. Met. Hard Mater 69 (2017) 66–109.

[29] P. Lied, et al., Comparison of K-dped and pure cold rolled tungsten sheets: tensile properties and brittle-to-ductile transition temperatures, J. Nucl. Mater. 544 (2021), 152664.

[30] S. Nogami, et al., Mechanical properties of tungsten: recent research on modified tungsten materials in, Japan J. Nucl. Mater. 543 (2020), 152506.

[31] A. Calvo, et al., Self-passivating tungsten alloys of the system W-Cr-Y for high temperature applications, Int. J. Refract. Hard Mater. 73 (2018) 29–37.

[32] A. Litnovsky, et al., Smart first wall materials for intrinsic safety of a fusion power plant, Fusion Eng. Des. 136 (2018) 878–882.

[33] A.v. Muller, et al., Melt infiltrated tungsten-copper composites as advanced heat sink materials for plasma facing components of future nuclear fusion devices, Fusion Eng. Des. 124 (2017) 455–459.

[34] E. Tejado, et al., Evolution of mechanical performance with temperature of W/Cu and W/CuCrZr composites for fusion heat sink applications, Mater. Sci. Eng.: A 712 (2018) 738–746.

[35] J. Reiser, et al., Ductilisation of tungsten (W): tungsten laminated composites, Int. J. Refract. Met. Hard Mater. 69 (2017) 66–109.

[36] A.v. Müller, et al., Tailored tungsten lattice structures for plasma facing components in magnetic confinement fusion devices, Mat. Today 39 (2020) 146–147.

[37] M. Richou, et al., Status on the W monoblock type high heat flux target with graded interlayer for application to DEMO divertor, Fusion Eng. Des. 124 (2017) 338–343.

[38] M. Richou etal., Performance assessment of thick W/Cu graded interlayer for DEMO divertor target, Fusion Eng. Des. 57 (2020) 111610.

[39] S. Roccella, et al., Ultrasonic test results before and after high heat flux testing on W-monoblock mock-ups of EU-DEMO vertical target, Fusion Eng. Des. 160 (2020), 111886.

[40] M. Galatanu, et al., Cu-based composites as thermal barrier materials in DEMO divertor components, Fusion Eng. Des. 124 (2017) 1131–1134.

[41] M. Galatanu, et al., Thermophysical properties of Cu-ZrO2 composites as potential thermal barrier materials for a DEMO W-monoblock divertor, Fusion Eng. Des. 127 (2018) 179–184.

[42] J. de Prado, et al., Microstructural and mechanical characterization of self-passivating W-Eurofer joints processed by brazing technique, Fusion Eng. Des. 169 (2021), 112496.

[43] R. Vila etal., Testing of neutron irradiated Silica optical windows for DEMO diagnostic and control. to be submitted to Proceedings of ICFRM 20.

[44] D. Cruz etal., Testing of 1 dpa neutron irradiated Alumina for DEMO applications, to be submitted to Proceedings of ICFRM 20.

[45] C. Yin, et al., Anisotropy in the hardness of single crystal tungsten before and after neutron irradiation, J. Nucl. Mater. 546 (2021), 152759.

[46] A. Zinovev, et al., Plastic deformation of ITER specification tungsten: temperature and strain rate dependent constitutive law deduced by inverse finite element analysis, Int. J. Refract. Metal. Hard Mater. 96 (2021), 105481.

[47] C. Yin, et al., Impact of neutron irradiation on hardening of baseline and advanced tungsten grades and its link to initial microstructure, Nucl. Fusion. 61 (2021), 066012.

[48] F. Balbaud, et al., A NEA review on innovative structural materials solutions, including advanced manufacturing processes for nuclear applications based on technology readiness assessment Nucl, Mater. ENERGY 27 (2021), 101006.

[49] A. Dubinko, et al., Microstructure and hardening induced by neutron irradiation in single crystal, ITER specification and cold rolled tungsten, Int. J. Refract. Met. Hard Mater 98 (2021), 105522.

[50] E. Gaganidze, et al., Fracture-mechanical properties of neutron irradiated ITER specification tungsten, J. Nucl. Mater. 547 (2021), 152761.

[51] M. Duerrschnabel, et al., New insights into microstructure of neutron-irradiated tungsten, Sci. Rep. 11 (2021).

[52] X. Chen, et al., Mechanical properties and microstructure characterization of Eurofer97 steel variants in EUROfusion program, Fusion Eng. Des. 146 (2019) 2227–2232.

[53] X. Chen, et al., Master curve fracture toughness characterization of Eurofer97 steel variants using miniature multi-notch bend bar specimens for fusion applications, in: _presented at the ASME 2019 Pressure Vessels & Piping Conference, San Antonio, Texas, USA, 2019.

[54] A. Bhattacharya etal., "Mechanical properties and microstructure characterization of unirradiated Eurofer-97 steel variants for the EUROfusion project," _ORNL/SPR-2018/882, 1471901, 2018.

[55] M. Rieth, et al., Technological aspects in blanket design: effects of micro-alloying and thermo-mechanical treatments of EUROFER97 type steels after neutron irradiation, Fusion Eng. Des. 168 (2021), 112645.

[56] D. Papadakis, et al., The competing effects of temperature and neutron irradiation on the microstructure and mechanical propertis of ITER grade tungsten, Fusion Eng. Des. 168 (2021), 112608.

[57] D. Terentyev, et al., Neutron irradiation hardening across ITER diverter tungsten armor, Int. J. Refract. Met. Hard Mater 95 (2021), 105437.

[58] S. Dellis, et al., Mechanical properties of neutron-irradiated single crystal tungsten W(100) studied by indentation and FEM modelling, J. Nucl. Mater. 551 (2021), 152985.

[59] G. Bonny, et al., Trends in vacancy distribution and hardness of high temperature neutron irradiated single crystal tungsten, Acta Mater. 198 (2020) 1–9.

[6] D. Terentyev, et al., Recent progress in the assessment of irradiation effects for in-vessel fusion materials. Tungsten and copper alloys, Nucl. Fusion. (2021) submitted.

[61] S. Nogami, et al., Neutron irradiation tolerance of potassium-doped and rhenium-alloyed tungsten, J. Nucl. Mater. 553 (2021), 153009.

[62] S.L. Dudarev, Density Functional Theory Models for Radiation Damage, Annu. Rev. Mater. Res. 43 (2013) 35–61.

[63] S.L. Dudarev, The non-Arrhenius migration of interstitial defects in bcc transition metals, C.R. Phys. 9 (2008) 409–417.

[64] R. Alexander, et al., Ab initio scaling laws for the formation energy of nanosized interstitial defect clusters in iron, tungsten, and vanadium, Phys. Rev. B 94 (2016), 024103.

[65] D.R. Mason, et al., Relaxation volumes of microscopic and mesoscopic irradiation-induced defects in tungsten, J. Appl. Phys. 126 (2019), 075112.

[66] D.R. Mason, et al., Observation of Transient and Asymptotic Driven Structural States of Tungsten Exposed to Radiation, Phys. Rev. Lett. 125 (2020), 225503.

[67] Pui-Wai Ma, et al., Universality of point defect structure in body-centered cubic metals, Phys. Rev. Materials 3 (2019), 013605.

[68] Pui-Wai Ma, et al., Nonuniversal structure of point defects in face-centered cubic metals, Phys. Rev. Materials 5 (2021), 013601.

[69] Pui-Wai Ma, et al., CALANIE: anisotropic elastic correction to the total energy, to mitigate the effect of periodic boundary conditions, Comput. Phys. Commun. 252 (2020), 107130.

[70] J. Wrobel, et al., Elastic dipole tensors and relaxation volumes of point defects in concentrated random magnetic Fe-Cr alloys, Comput. Mater. Sci. 194 (2021), 110435.

[71] L. Vegard, Die Konstitution der Mischkristalle und die Raumfüllung der Atome, Zeitschrift für Physik 5 (1921) 17–26, https://doi.org/10.1007/BF01349680.

[72] J.B.J. Chapman, et al., Dynamics of magnetism in Fe-Cr alloys with Cr clustering, Phys. Rev. B 99 (2019), 184413.

[73] K. Mergia, et al., Phase stability of Fe-5at%Cr and Fe-10at%Cr films under Fe+ ion irradiation, J. Phys.: Condens. Matter 32 (2020), 185702.

[74] A. Bhattacharya, et al., Chromium enrichment on the habit plane of dislocation loops in ion-irradiated high-purity Fe-Cr alloys, Acta Mater 78 (2014) 394–403.

[75] J.-.L. Boutard, A. Alamo, R. Lindau, M. Rieth, Fissile core and Tritium-Breeding Blanket: structural materials and their requirements, C.R. Phys. 9 (2008) 287–302.

[76] K. Nordlund, et al., Primary radiation damage: a review of current understanding and models, J. Nucl. Mater. 512 (2018) 450–479.

[77] F. Granberg, et al., Defect accumulation and evolution during prolonged irradiation of Fe and FeCr alloys, J. Nucl. Mater. 528 (2020), 151843.

[78] E. Levo, et al., Temperature effect on irradiation damage in equiatomic multi-component alloys, Comput. Mater. Sci. 197 (2021), 110571.

[79] S.J. Zinkle, et al., Designing Radiation Resistance in Materials for Fusion Energy, Annu. Rev. Mater. Res. 44 (2014) 241.

[80] P.M. Derlet, et al., Microscopic structure of a heavily irradiated material, Phys. Rev. Materials 4 (2020), 023605.

[81] G.R. Odette, R.K. Nanstad, Predictive reactor pressure vessel steel irradiation embrittlement models: issues and opportunities, JOM 61 (2009) 17–23, issue 7.

[82] E. Gaganidze, et al., Mechanical properties and TEM examination of RAFM steels irradiated up to 70 dpa in BOR-60, J. Nucl. Mater. 417 (2011) 93–98.

[83] F.A. Garner, M.B. Toloczko, B.H. Sencer, Comparison of swelling and irradiation creep behavior of fcc-austenitic and bcc-ferritic/martensitic alloys at high neutron exposure, J. Nucl. Mater. 276 (2000) 123–142.

[84] E. Meslin, M. Lambrecht, M. Hernández-Mayoral, F. Bergner, L. Malerba, P. Pareige, B. Radiguet, A. Barbu, D. Gómez-Briceño, A. Ulbricht, A. Almazouzi, Characterization of neutron-irradiated ferritic model alloys and a RPV steel from combined APT, SANS, TEM and PAS analyses, J. Nucl. Mater. 406 (2010) 73–83.

[85] B. Tyburska, V. Kh. Alimov, O.V. Ogorodnikova, K. Schmid, K. Ertl, Deuterium retention in self-damaged tungsten, J. Nucl. Mater. 395 (2009) 150–155.

[86] J. Wang, Y. Hatano, T. Hinoki, V. Kh. Alimov, A.V. Spitsyn, N.P. Bobyr, S. Kondo, T. Toyama, H.T. Lee, Y. Ueda, T. Schwarz-Selinger, Deuterium retention in W and binary W alloys irradiated with high energy Fe ions, J. Nucl. Mater. 545 (2021), 152749.

[87] B. Wielunska, et al., D retention in self-damaged tungsten versus damage level, in: Proceedings of the PFMC-18 conference, Juelich, Germany, 2021.

[88] D.R. Mason, et al., Parameter-free quantitative simulation of high dose microstructure and hydrogen retention in ion-irradiated tungsten, Phys. Rev. Materials (2021) submitted for publication.

[89] S.L. Dudarev, et al., A multi-scale model for stresses, strains and swelling of reactor components under irradiation, Nucl. Fusion. 58 (2018), 126002.

[90] L. Reali, et al., Macroscopic elastic stress and strain produced by irradiation, Nucl. Fusion (2021) submitted for publication.

[91] S. Sato, K. Maki, Analytical representation for neutron streaming through slits in fusion reactor blanket by Monte Carlo calculation, Fusion Eng. Des. 65 (2003) 501–524.

[92] M.R. Gilbert, S.L. Dudarev, D. Nguyen-Manh, S. Zheng, L.W. Packer, J.-Ch. Sublet, Neutron-induced dpa, transmutations, gas production, and helium embrittlement of fusion materials, J. Nucl. Mater. 442 (2013) S755–S760.

[93] R.A. Holt, Mechanisms of irradiation growth of alpha zirconium alloys, J. Nucl. Mater. 159 (1988) 310–338.

[94] A. Bhattacharya etal., Cavity swelling in irradiated materials, In: Konings, Rudy JM and Stoller Roger E (eds.) Comprehensive Nuclear Materials 2nd edition, vol. 1, pp. 406–455. Oxford: Elsevier.

[95] M. Klimenkov, et al., Post-irradiation microstructural examination of EUROFER-ODS steel irradiated at 300°C and 400°C, J. Nucl. Mater. (2021) accepted for publication.

[96] S.L. Dudarev, P.-.W. Ma, Elastic fields, dipole tensors, and interaction between self-interstitial atom defects in bcc transition metals, Phys. Rev. Materials 2 (2018), 033602.

[97] F.A. Garner, Radiation-induced damage in austenitic structural steels used in nuclear reactors, Konings, R. J. M. and Stoller R. E. (Eds.), in: Comprehensive Nuclear Materials, 2nd edition, 3, Elsevier, Oxford, 2020, pp. 57–168.

[98] F. Hofmann etal., Non-contact measurement of thermal diffusivity in ion-implanted nuclear materials, Sci. Reports, 5 (2015)16042.

[99] G. Federici etal., The EU DEMO staged design approach in the Pre-concept design phase, this issue.